A Chirality-Based Quantum Leap:
A Forward-Looking Review

Clarice D. Aiello,[*,†,‡] Muneer Abbas,[¶] John Abendroth,[§] Amartya S. Banerjee,[‖,†] David Beratan,[⊥] Jason Belling,[†,#] Bertrand Berche,[@] Antia Botana,[△] Justin R. Caram,[#] Luca Celardo,[▽] Gianaurelio Cuniberti,[††] Arezoo Dianat,[††] Yuqi Guo,[‡‡] Rafael Gutierrez,[††] Carmen Herrmann,[¶¶] Josh Hihath,[§§] Suneet Kale,[‖‖] Philip Kurian,[⊥⊥] Ying-Cheng Lai,[##] Ernesto Medina,[@@] Vladimiro Mujica,[‖‖] Ron Naaman,[△△] Mohammadreza Noormandipour,[†,‡] Julio Palma,[▽▽] Yossi Paltiel,[†††] William Petuskey,[‖‖] João Carlos Ribeiro-Silva,[‡‡‡] Dominik Stemer,[†,‖] Ana Valdes-Curiel,[†,‡] Solmar Varela,[¶¶] David Waldeck,[§§§] Paul S. Weiss,[†,‖] Helmut Zacharias,[‖‖‖‖] and Qing Hua Wang[*,‡‡]

E-mail: cla@ucla.edu; qhwang@asu.edu

† California NanoSystems Institute, University of California, Los Angeles, Los Angeles, CA, USA, 90095

‡ Department of Electrical and Computer Engineering, University of California, Los Angeles, Los Angeles, CA, USA, 90095

¶ Department of Microbiology, Howard University, Washington, DC, USA, 20059

§ Department of Materials Science and Engineering, Stanford University, Stanford, CA, USA, 94305

‖ Department of Materials Science and Engineering, University of California, Los Angeles, Los Angeles, CA, USA, 90095

$^{\perp}$ Department of Chemistry, Duke University, Durham, NC, USA, 27708

$^{\#}$ Department of Chemistry & Biochemistry, University of California, Los Angeles, Los Angeles, CA, USA, 90095

$^{@}$ Laboratoire de Physique et Chimie Thoriques, UMR Université de Lorraine-CNRS, 7019 54506 Vanduvre les Nancy, France

$^{\triangle}$ Department of Physics, Arizona State University, Tempe, AZ, USA, 85287

$^{\nabla}$ Institute of Physics, IFUAP-BUAP, 72000 Puebla, Mexico

†† Institute for Materials Science and Max Bergmann Center of Biomaterials, Dresden University of Technology, 01062 Dresden, Germany

‡‡ School for Engineering of Matter, Transport and Energy, Arizona State University, Tempe, AZ, USA, 85287

¶¶ Department of Chemistry, University of Hamburg, 20146 Hamburg, Germany

§§ Department of Electrical and Computer Engineering, University of California, Davis, Davis, CA, USA, 95616

$^{\|\|}$ School of Molecular Sciences, Arizona State University, Tempe, AZ, USA, 85287

$^{\perp\perp}$ Graduate School, Howard University, Washington, DC, USA 20059

$^{\#\#}$ School of Electrical, Computer and Energy Engineering, Arizona State University, Tempe, AZ, USA, 85287

$^{@@}$ School of Physical Sciences & Nanotechnology, Yachay Tech University, 100119-Urcuqu, Ecuador

$^{\triangle\triangle}$ Department of Chemical and Biological Physics, Weizmann Institute of Science, Rehovot 76100, Israel

$^{\nabla\nabla}$ Department of Chemistry, Pennsylvania State University, Lemont Furnace, PA, USA, 15456

††† Applied Physics Department and the Center for Nano-Science and Nano-Technology, Hebrew University of Jerusalem, Jerusalem 91904, Israel

‡‡‡ Laboratory of Genetics and Molecular Cardiology, Heart Institute, University of São

Paulo Medical School, São Paulo, Brazil

¶¶¶ School of Chemical Sciences & Engineering, Yachay Tech University, 100119- Urcuquí, Ecuador

§§§ Department of Chemistry, University of Pittsburgh, Pittsburgh, PA, USA, 15260

‖‖‖ Center for Soft Nanoscience, University of Mnster, 48149 Mnster, Germany

* Authors to whom correspondence should be addressed

Abstract

The interest in chiral degrees of freedom occurring in matter and in electromagnetic fields is experiencing a renaissance driven by recent observations of the chiral-induced spin selectivity (CISS) effect in chiral molecules and engineered nanomaterials. The CISS effect underpins the fact that charge transport through nanoscopic chiral structures has been conclusively shown to favor a particular electronic spin orientation, resulting in large room-temperature spin polarizations. Observations of the CISS effect suggest unique opportunities for spin control and for the design and fabrication of room-temperature quantum devices from the bottom up, with atomic-scale precision. Any technology that relies on optimal charge transport – *i.e.*, the entire quantum device industry – could benefit from chiral quantum properties. These can be theoretically and experimentally investigated from a quantum information perspective, which is presently lacking. There are uncharted implications for the quantum sciences once chiral couplings can be engineered to affect how well quantum information is stored, transduced and manipulated. This forward-looking review article provides a survey of the experimental and theoretical fundamentals of chiral-influenced quantum effects, and presents a vision for their future role in enabling room-temperature quantum technologies.

Contents

1   Overview

1.1   Quantum Effects in Chiral Matter

Chiral matter (*i.e.*, structures that can occur with left- or right-handed non-superimposable symmetry) offers unparalleled opportunities for the exquisite control of electron and spin transport due to its unique optical, electric and magnetic properties. These properties are often observed at near-room temperatures, and suggest that quantum devices based on chiral matter can operate similarly, if properly designed. In this forward-looking review, we stress the potentiality of chiral matter and fields, in particular with respect to their hitherto little explored applications in the quantum sciences. We detail how chiral matter presents advantages for: the scalability and flexibility of molecular architectures interfaced with low-dimensional materials; the transferring of spin information content from electrons to nuclei; the operating of quantum devices at room temperature and in noisy photonic, phononic and electronic environments; and the furthering of investigations into the emergent field of quantum biology.

In particular, the chiral-induced spin selectivity (CISS) effect is an unusual semiconduc-

tor-like behavior first observed in biological structures, and only later replicated in technological applications, existing even in diamagnetic systems. It describes the fact that, at room temperature, charge transport through nanoscopic chiral structures favors a particular component of an electron spin in the direction of propagation – an effect also referred to as 'spin polarization' – all in the absence of external magnetic fields.

The CISS effect can be physically understood as an electron scattering process in a molecular potential where spin-orbit interaction is taken into account and where both space inversion and time reversal symmetries are broken. This combination of physical constraints translates into spin polarization and spin filtering arising from the transmission probabilities for the two spin components being different. Chiral molecules and chiral materials can be controlled to act as both spin polarizers and filters depending on molecular design variables. The presence of the CISS effect has been established in processes associated with electron transfer, electron transport, and bond polarization through chiral centers or complex helical chiral structures.

In technological quantum devices, achieving spin polarization is not trivial and requires a sophisticated degree of 'quantum control' via tailored electromagnetic excitation. Nature seems to have found its own way towards spin polarization. As a consequence of the CISS effect, chiral isomers (*i.e.*, enantiomers) have opposite electron spin orientation preferences, which might be explored by the pharmaceutical industry. CISS might also have tremendous biological implications, as proteins and many biomolecules, including DNA, are chiral. Finally, it was recently demonstrated that electron transport through the surface of bacteria is spin-polarized. If spin is harnessed in cellular electron transport processes it opens the door for quantum information transfer in living environments. In addition, electron transfer through chiral structures is more efficient than that through comparable achiral structures, and under some conditions can be temperature-independent – both features being relevant to all technologies relying on optimal charge transport (*i.e.*, the whole quantum device industry). Finally, the complex responses of chiral molecules to electromagnetic fields, involving

both the electric and magnetic polarizabilities, pave the way to control and to manipulate interactions and the imprinting of chiral characteristics onto photons, phonons and materials.

Unveiling the quantum mechanisms behind electron spin transport via CISS will allow the manipulation of the effect to be used for technological and therapeutic advantage – especially in the quantum sciences – as we aim to demonstrate with this review.

1.2 Outline of Review

We will review fundamental theoretical and experimental aspects of quantum effects in chiral materials in sections organized as follows:

- In **Section** 2, we present a comprehensive picture of a broad variety of measurement results that have been obtained in connection with the CISS effect;

- In **Section** 3, theoretical predictions and modelling tools that inform the understanding of CISS are described;

- In **Section** 4, we detail groundbreaking material design strategies that are being developed to engineer and tune CISS;

- In **Section** 5, we review potential chirality-mediated effects in biology, and predict potential future applications in the field;

- In **Section** 6, we explore the interaction of matter and electromagnetic fields via chiral degrees of freedom;

- In **Section** 7, we propose forward-looking applications of the CISS effect in the quantum sciences.

This comprehensive review attests to the tremendous potential of harnessing CISS as a tool in fields as diverse as spintronics, nanotechnology, besides towards the control of biological systems at the nanoscale. Importantly, these advances in our understanding and

observations of chirality-based quantum phenomena are poised to be incorporated into a new phase of spin-based quantum technologies working at elevated, near-room temperatures.

2 Chirality and Spin measurements

2.1 Electrochemistry Experiments

In electrochemical processes, electrons are either removed or added to a chemical system. As shown schematically in **Fig. 1**, the redox process of chiral molecules can be spin-selective. When an electron is approaching a chiral molecule, it induces charge polarization in the molecule. As a result, an induced electric dipole is formed and the electron is attracted to the positive pole. It was shown that in chiral molecules, charge polarization is accompanied by spin polarization, due to the CISS effect,[1] and which spin is associated with which electric pole depends on the handedness of the molecule. Therefore, when spin-polarized electrons approach a chiral system,[2] its probability to attach to the molecule is higher if the spin on the positive pole is polarized opposite to the spin of the approaching electron. This restriction results in enantioselectivity that is a consequence of the electron being spin polarized.[3]

Recently, it was demonstrated that spin selectivity can control both reduction and oxidation electrochemical processes.[4] As an example for an oxidation process, electropolymerization of 1-pyrenecarboxylic acid was performed on a magnetic electrode (10 nm of Ni and 10 nm of Au on ITO) that was magnetized either 'up' or 'down' relative to the electrode surface. **Fig. 2a** shows a reaction scheme for the formation of polypyrene. Initiation of the reaction involves electrooxidation of the monomer unit to form a radical cation. The steric constraints of the pyrene rings lead to a propeller-like arrangement of the monomers; control over their stereoarrangement imparts axial chirality into the polymer chain. **Fig. 2b** shows the circular dichroism (CD) spectra taken of the pyrene polymer films on the electrode surface. In turn, the red curve shows the CD spectrum with the electrode magnetized in the 'up' direction and the blue curve corresponds to the case for magnetization in the 'down' direction. The
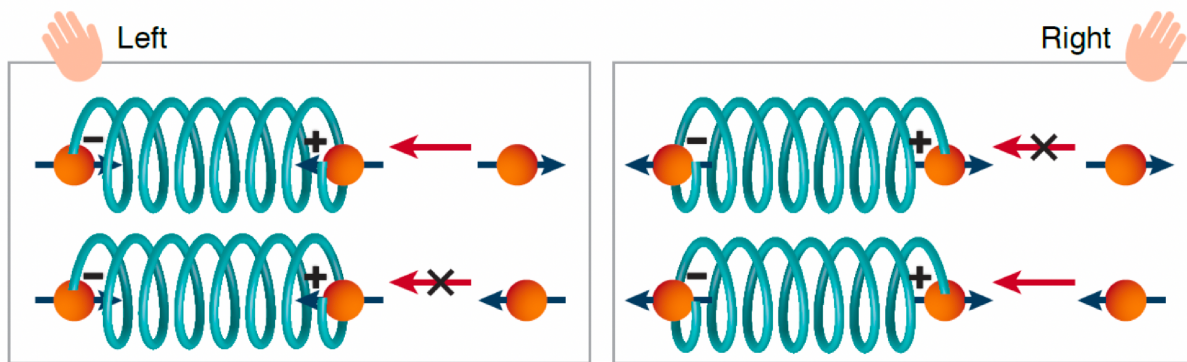
Fig. 1: Illustration of a spin polarization-induced enantioselective reaction mechanism. When an electron approaches a chiral molecule, charge rearrangement occurs and the molecule becomes charge polarized with the electron attracted to the positive pole of the molecule. Depending upon the molecules handedness (left-handed or right-handed) and the spin orientation of the electron, the interaction is more favored or less favored for a given spin polarization. Reproduced with permission from Ref. 3. Copyright 2020 by the Royal Society of Chemistry.

red and blue curves exhibit opposite Cotton effects in pyrene's excimer spectral region.

The chirality of the polymer-coated electrode was confirmed by performing cyclic voltammetry with a chiral ferrocene (Fc) redox couple. **Fig. 2c** shows voltammetry data collected using the polypyrene-coated films as working electrodes for two different enantiomerically pure solutions of chiral ferrocene: (S)-Fc (black) and (R)-Fc (red). It is evident from the voltammetric peak currents that the 'up' grown electrode is more sensitive to the (S)-Fc, whereas the 'down' grown electrode is more sensitive to the (R)-Fc. Similar dependencies for redox properties with chiral working electrodes have been reported previously, and further corroborate the chirality demonstrated in the circular dichroism measurements.This result demonstrates how chiral spin transport can lead to highly amplified downstream chemical products.[5]

Spin-related effects have also been observed in cyclic voltammetry (CV) experiments performed under an applied magnetic field on a non-ferromagnetic electrode modified with a thin electroactive oligothiophene film.[6] When flipping the magnet's north/south orientation, the CV peaks of two achiral, chemically reversible Fe(III)/Fe(II) redox couples in aqueous
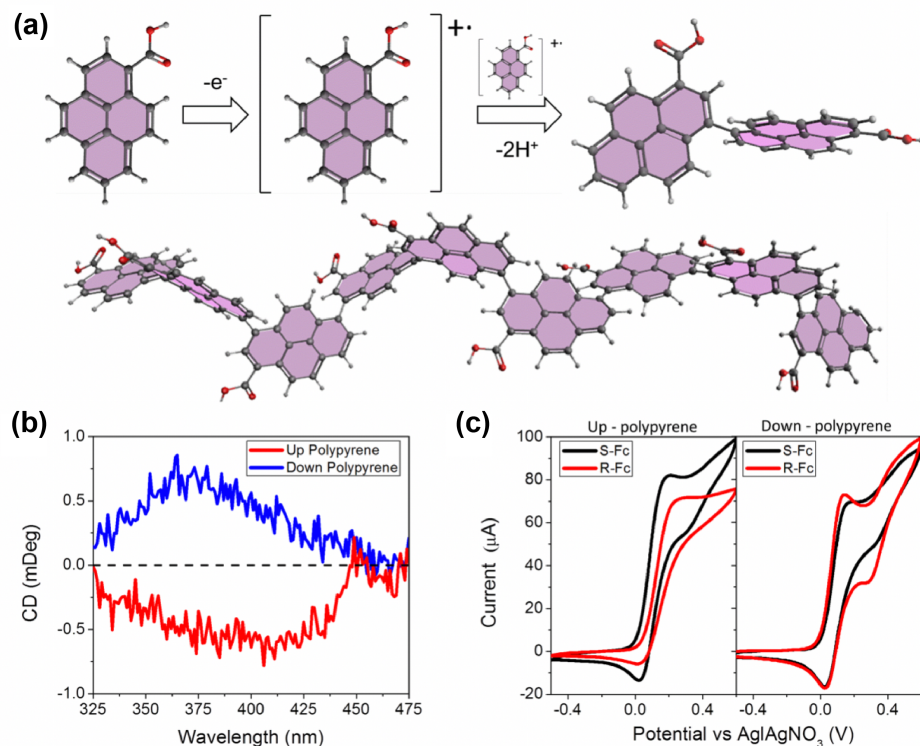
Fig. 2: Reaction scheme and chirality in electropolymerized polypyrene. (a) Reaction scheme for the polymerization of 1-pyrenecarboxcylic acids into polypyrene which exhibits a helical twist (see main text for more details). **(b)** Circular dichroism spectra for electrodes coated with polypyrene where a magnetic field was applied Up (red) or Down (blue) during electropolymerization. **(c)** Electrochemistry measurements on (S)- (black) or (R)-ferrocene (red) with the Up (left) or Down (right) polypyrene-coated working electrodes. Reproduced with permission from Ref. 4. Copyright 2020 by John Wiley and Sons.

or organic solution undergo impressive potential shifts (up to nearly 0.5 V depending on protocol conditions), by changing the film's (R)- or (S)-configuration. This observed effect is another manifestation of the spin-chirality relation in electrochemical processes.

2.2 Enantioseparation Experiments

The relation between spin and chirality via the CISS phenomenon naturally leads to consider the possible interaction between chiral molecules and ferromagnetic surfaces.[7–11] This interaction should be spin sensitive due to short-range magnetic exchange interactions- as chiral molecules approach the surface, charge reorganization and spin polarization, which

depend on the handedness of the molecules, should take place. We refer below to two specific examples of this mechanism:

i) It has recently been demonstrated that magnetization switching of ferromagnetic thin layers can be induced solely by adsorption of chiral molecules without external magnetic fields or spin polarized currents.[9] The mechanism by which chiral molecules can induce the magnetization switching is shown in **Fig. 3**. The effect of adsorbed chiral molecules on the properties of a ferromagnetic substrate has been demonstrated by studying the adsorption of L- and D-oligopeptides a on a thin ferromagnetic film, with magnetization not initially defined. The direction of the magnetization depends on the handedness of the adsorbed chiral molecules. Importantly, less than 10^{13} electrons per cm^2 are sufficient to induce a reversal of the magnetization on the ferromagnetic layer in the direction perpendicular to the surface (the current density required for common mechanisms in modern magnetoresistive random access memory such as spin-transfer torque, is 10^{25} electrons per cm^2). The high efficiency of magnetization results from the molecule-substrate exchange interaction. As such, this concept could be used to achieve simple surface spintronic logic devices.
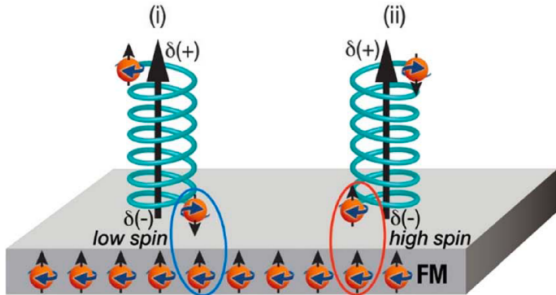
Fig. 3: Chiral-induced spin selectivity effect and ferromagnetic substrates. As a chiral molecule approaches the ferromagnetic (FM) substrate, its charge polarization generates a spin polarization at the two ends of the molecule. For a specific enantiomer, the interaction between the magnetized surface and the molecule (circled in blue and red) follows a low-spin or a high-spin potential, depending on the direction of magnetization of the substrate. Reproduced with permission from Ref. 10. Copyright 2018 by The American Association for the Advancement of Science.

ii) Conversely, it has been shown that enantiomers can be separated by adsorbing them on a ferromagnetic substrate with magnetization perpendicular to the surface.[10] Unambigu-

ous enantioselectivity on a ferromagnetic substrate has been obtained for a variety of chiral molecules and magnetic substrates. Namely, while one enantiomer adsorbs faster when the magnetic dipole is pointing up, the other adsorbs faster when the substrate is magnetized in the opposite direction. The interaction between the chiral molecules and the magnetized substrate is not affected by the magnetic field but by the interaction between the spin-polarized molecule and the spin of the electrons on the substrate. As above, the effect is associated with the magnetic-exchange interaction of the spin-polarized molecules with the spin-polarized substrate. This phenomenon opens up prospects for a novel and generic approach to enantiomeric separations, which are critically important to the chemical industry.

2.3 Molecular Electronics Experiments

Naaman and co-workers reported a large asymmetry in the transmission probabilities of polarized electrons by thin films of chiral molecules.[12] This was supported by electron transmission experiments through chiral monolayers using scanning tunneling microscopy (STM) demonstrating that chiral systems can act as spin filters and spin polarizers,[13,14] allowing the preferential transmission of only one spin component. Theory indicates that this is possible due to enhanced spin-orbit interactions and a space and time reversal symmetry breaking – the result of transport through chiral symmetries and an electrochemical gradient induced through an external voltage or a free energy gradient.[15,16]

Break-junction devices provide an alternative class of measurements that utilize nanostructured, moveable electrodes to make contact to a single molecule to study the charge transport properties.[17–20] In this system, two electrodes are brought into and out of contact in the presence of the molecules of interest. As the two electrodes are withdrawn the current is measured. When a molecule binds between the two electrodes a plateau is observed in the current vs. distance trace, and by measuring thousands of these traces it is possible to statistically determine the conductance of a single-molecule junction. These systems have been used extensively for studying charge transport in chiral molecules such as DNA,[21–25]

RNA,[26,27] PNA,[28] peptides,[29,30] and proteins,[31,32] and have been utilized to explore spin-selectivity in a variety of molecules in recent years by either applying a magnetic field or using a spin-polarized electrode to inject specified spins.[33,34]

Recently, these approaches have been combined to explore spin-selectivity in a diamagnetic, helical peptide chain which formed an α-helix.[13] These experiments allow measurement of the spin polarization power of a chiral molecule and provide direct evidence of the spin-filtering capabilities of these systems. By changing both the chirality of the molecule (by using both L- and D- isomers) and the magnetization orientation of the injecting electrode, they were able to demonstrate a clear change in the charge transport properties of the molecular system through these four iterations, and determine a spin polarization power (capability to spinpolarize electrical current) of 60%.

Moving forward in this area suggests that nucleic acid-based systems may provide a fruitful framework for understanding CISS behavior at the single-molecule level as there is a large variety of conductance measurements on these molecules,[21–25] synthetic approaches will allow facile control over both the length and helical pitch of the molecules, and although there can be some structural changes when DNA is dehydrated,[35–37] the helices can survive both vacuum and wide-temperature ranges.[38]

The conductive probe and spin-exchange methods used to test spin-dependent transport or charge redistribution involve multiple contacts or molecules within an interface, which may convolute spin-selective tunneling effects across individual chiral molecule bridges. Alternatively, scanning tunneling microscopy break junction (STM-BJ) techniques provide a measurement of conductance through single molecules, enabling hundreds to thousands of measurements for statistically relevant analyses. Using a spin-polarized STM-BJ method, Aragonès *et al.* demonstrated that conductance between ferromagnetic Ni tips and Au surfaces bridged by sulfur-terminated α-helical peptides (cysteine residues) depended on tip magnetization direction and handedness (L or D) of aminoacid residues,[13] as shown in **Fig. 4**. The results highlight a direct correlation between electron spin polarization and transport.

Still, experimental evidence is lacking that can unambiguously distinguish incoherent hopping from coherent tunneling in spin-dependent conductance through the chiral molecular framework. Moving forward, systematic investigation of the dependence of monomer sequence, length, and molecular dipole on conductance using spin-polarized STM-BJ techniques could be used to categorize spin filtering due to the CISS effect in this transport regime.[39]
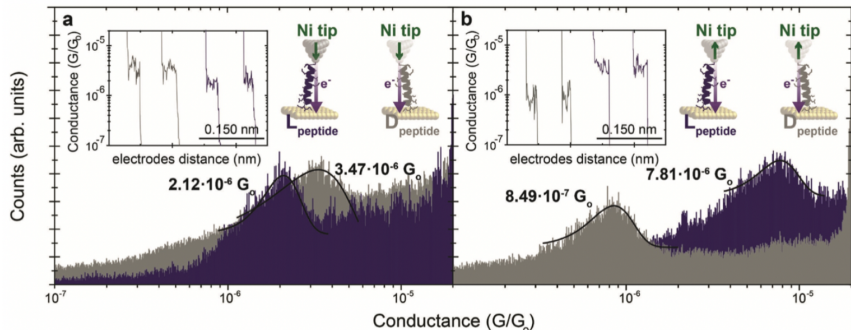
Fig. 4: Single-peptide conductance histograms from scanning tunneling microscopy break-junction measurements with Ni tips magnetized. **a)** down and **b)** up for left- versus right-handed alpha-helical peptides composed of 22 amino acid residues bridges attached to gold substrates. Insets depict representative current versus pulling traces with well-defined single-molecule plateau features. Conductance values were extracted from Gaussian fits to the histograms. Adapted with permission from Ref. 13. Copyright 2017 by John Wiley and Sons.

2.4   Scanning Probe Microscopy Experiments

Direct methods of studying spin-selective conductive properties of self-assembled monolayers (SAMs) of chiral molecules using scanning probes have been employed with great success over the past 10 years. In the first experimental demonstration of this methodology, Xie *et al.* utilized conductive atomic force microscopy (c-AFM) to measure room temperature magnetization-dependent conductivity through Au-nanoparticle-terminated SAMs of double-stranded DNA (ds-DNA) on thin film Ni.[40] Although the variance between individual measurements is significant, likely due to local variations in electrical contact between the AFM tip and the Au NP, comparison of current-voltage traces collected under these varying

14

conditions reveals a clear asymmetry in the Ni-DNA-AuNP junction conductivity, dependent on the magnetization orientation of the Ni substrate, thereby revealing a preference for electrons with their spin aligned parallel to momentum in tunneling transport through right-handed dsDNA. Control measurements conducted with Au instead of Ni thin films confirm the conduction asymmetry to be predicated on the presence of both a source/sink of spin-polarized electrons (the magnetic thin film), and a spin-discriminating conductive element (the ds-DNA). This behavior starkly contrasts that of standard organic spin valves, in which organic layers typically take the role of weakly-interacting non-magnetic spacing layers, carrying spin-polarized electrons from one magnetized material to another.[41,42] Instead, the chiral ds-DNA layer behaves as an active element, more similar to a traditional inorganic spin valve. Mishra *et al.* have recently utilized a similar approach to study length-dependent spin-selectivity in conduction through SAMs of ds-DNA and α-helical peptides.[43]

Although the application of SAM-based surface modification methods to reactive metal thin films such as Ni have been demonstrated,[45] the formation of SAMs on reactive surfaces is known to be complicated by competitive formation of surface oxide layers, which may displace molecules, limit molecular adsorption, and worsen film uniformity.[46] In the context of chiral spintronics, this challenge has traditionally been overcome through the use of a thin inert capping layer, such as Au, which protects the magnetic layer from oxidation.[47–49] However, the capping layer must be carefully implemented; thicker capping layers of Au, which as a heavy element induces strong spin-orbit coupling effects in conducted electrons, have been shown to lead to spin randomization and nullification of spin-dependent effects in charge transport through the chiral molecules assembled thereupon.[50,51] The capacity to apply c-AFM to characterize conduction in chiral molecular films without the need for a capping layer, as exhibited by magnetic c-AFM (mc-AFM), is therefore highly desirable.

Bloom and colleagues applied mc-AFM to study spin-selective conduction through chiral CdSe quantum dots (QDs) drop cast onto highly ordered pyrolytic graphite (HOPG).[52] When functionalized with chiral ligands, QDs demonstrate strong chiroptical activity as a result
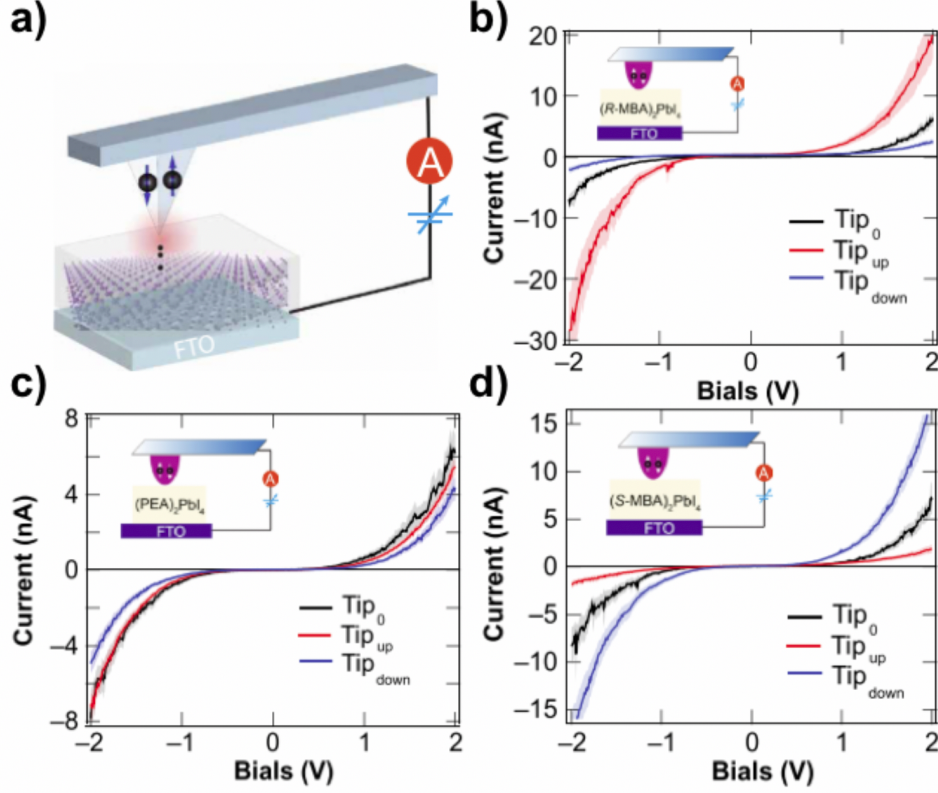
Fig. 5: (a) Magnetic conductive atomic force microscopy measurement of chiral perovskite thin film experimental schematic. **(b)-(d)** Current voltage traces collected for thin films of lead-iodide perovskites containing chiral R-methylbenzylammonium, achiral phenylmethylamine, and chiral S-methylbenzylammonium, respectively, as a function of tip-magnetization orientation. Reproduced with permission from Ref. 44. Copyright 2019 by the American Association for the Advancement of Science.

of orbital hybridization between the highest occupied molecular orbitals of the chiral ligand and the valence band states of the QDs.[53] In analogous measurements to those conducted by Xie *et al.*, Bloom and colleagues characterized the conductivity of these hybrid QD-chiral molecule junctions as a function of Co-Cr mc-AFM tip magnetization orientation. Once again, a distinct asymmetry is apparent when comparing current-voltage traces collected for QDs functionalized with L- vs. D-cysteine ligands. Tip magnetization persistence was confirmed by comparing magnetic force microscopy images collected of a hard drive before and after sample analysis.

Subsequent applications of mc-AFM have moved beyond chiral QDs toward characterizing spin-selective conductivity through thicker films of ordered chiral materials. Lu *et al.*

have reported remarkable conduction asymmetries of up to 86% (measured as percent difference in current at 2V for 'tip-up' and 'tip-down' magnetization conditions) in solution processed 50 nm thin films of lead-iodide hybrid perovskites, as shown in **Fig. 5**.[44] Similar values of spin-selectivity have recently been reported in c-AFM measurements of conduction through supramolecular chiral nanofibers assembled on Ni thin films capped with gold.[54] By tuning the chirality (R- or S-) of the organic methylbenzylammonium constituent, Lu and colleagues demonstrated control over the handedness of the perovskite films studied. More recent reports focusing on similar tin-iodide perovskites have yielded even higher spin-selectivity values,[55] nearing 94% and underscoring the value of conductive probe microscopy as a powerful tool for rapid and direct characterization of novel phenomena in chiral materials, particularly as they continue to grow in relevance for the broader spintronics community.

2.5   Spin Exchange Microscopy Experiments

Another scanning probe method that instead relies on non-ferromagnetic tips functionalized with chiral molecules has enabled local magnetic imaging similar to magnetic exchange force microscopy.[56] Ziv *et al.* showed that transient spin polarization accompanying charge redistribution due to the CISS effect in the chiral molecules enabled spin exchange interactions with magnetized samples, distinguishing domains magnetized up vs down by different forces exerted on the AFM cantilevers close to the sample surfaces.[2] The different forces were hypothesized to be a result of either symmetric or anti-symmetric spin alignment in wavefunction overlap between the molecules on the tips and the magnetized sample. Similarly, recent Kelvin-probe force microscopy measurements by Ghosh *et al.* on ferromagnetic films coated with chiral SAMs revealed electron spin-dependent charge penetration across the molecular interface.[51] This dependence of wavefunction overlap between magnetized materials and chiral molecules on the spin-exchange interaction could be exploited for proximity-induced magnetization[9] and enantiomer separations[10] that occur upon molecular adsorption, or rationalize spin-selective contributions to stereoselective interactions between

biomolecules resulting from induced dipole-dipole interactions.[1]

2.6 Experiments Involving Superconductivity

Spin-selective transport through chiral molecules has also shown unusual conduction phenomena near superconducting interfaces. In particular, chiral α-helical polyaniline molecules that are in proximity to niobium superconductors through chemisorption on metallic layers demonstrate unconventional superconductivity. Shapira *et al.* used scanning tunneling spectroscopy to analyze a multilayered polyaniline-gold bilayer-niobium substrate and observed zero-bias conductance peaks embedded inside a gap from the tunneling spectra.[57] This zero-bias peak reduced in the presence of a magnetic field but did not split, inferring an unconventional order parameter that is consistent with equal-spin triplet pairing p-wave symmetry. In comparison, the adsorption of non-helical chiral cysteine molecules demonstrated no change in the order parameter.

Similarly, junctions of superconducting niobium and metallic films bridged by chiral α-helical polyaniline induced p-wave order-parameters demonstrating phase-coherent transport through chiral organic films.[59] Alpern *et al.* further analyzed the proximity effects of chiral films in multilayered superconducting systems and observed that chemically adsorbed alpha-helix polyalanine can induce magnetic-like state behavior. Specifically, in-gap states were observed that were nearly symmetrical around a zero-conduction bias that closely resembled Yu-Shiba Rusinov states,[58] see **Fig. 6**.

Collectively, these observations provide evidence that chiral molecules can behave as magnetic impurities when in proximity to superconductors enabling a wide range of applications of spin-selective transport through superconducting films.

3 Chirality and Spin Theory

The CISS effect has been confirmed by a range of different experimental methods and for a
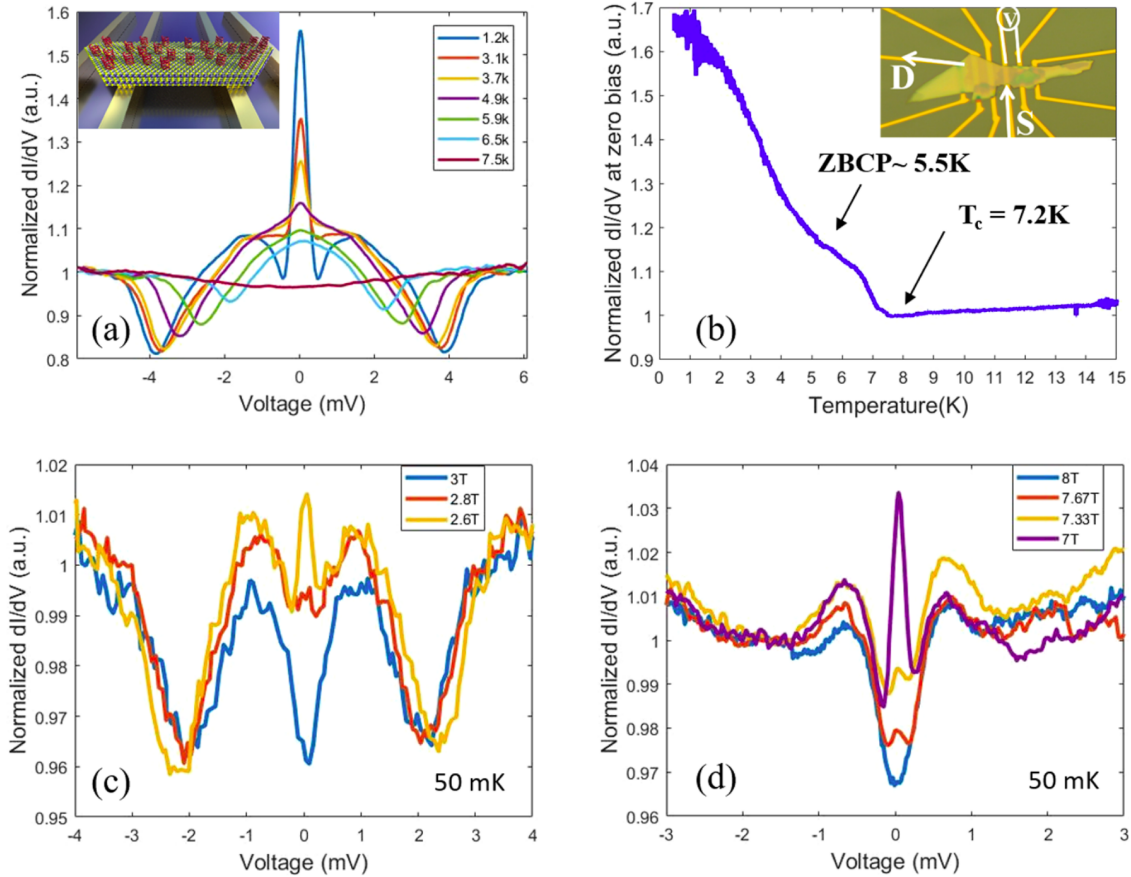
Fig. 6: Conductance properties of a low resistance (120Ω) NbSe$_2$/Au junction after chemisorption of chiral molecules on the NbSe$_2$ flake ($\sim$ 25 nm-thick). (a) Temperature dependence of dI/dV vs. V spectra showing a distinct ZBCP that vanishes at higher temperatures (but still below T$_c$). Inset: Illustration of a chiral-molecules/NbSe$_2$-flake/Au sample. **(b)** Temperature dependence of the conductance at zero bias with two transition temperatures marked by arrows: T$_c$ = 7.2 K, where the zero bias conductance starts to rise due to the Andreev dome and 5.5 K where a ZBCP starts to appear. Inset: Optical image of the sample with the measurement scheme depicted. **(c,d)** Perpendicular **(c)** and parallel **(d)** magnetic field dependencies of the conductance spectrum, showing that in high magnetic fields, yet below the parallel and perpendicular critical fields (H$_{c_2}$)of bulk NbSe$_2$, the ZBCP vanishes, revealing an underlying gap. Reproduced with permission from Ref. 58. Copyright 2019 by the American Chemical Society.

wide range of chiral molecules and materials. Our current understanding of the CISS effect is that it is a room-temperature magnetic response due to internal molecular fields generated by electron spin-orbit interaction in chiral systems. This effect survives the inclusion of many-electron interactions and can co-exist with other magnetic responses, including triplet radical formation, interstate crossing and singlet fission, which provides a fertile ground for

spin manipulation. This effect is closely related to exchange interactions, which play a vital role in molecular recognition and chirality induced effects on magnetic surfaces.

The spin-orbit coupling that provides a source of magnetic fields for electrons in an atom is a relativistic effect and is thus weak: on the order of a few meV. However, it is still possible to generate a sizable spin polarization through cumulative interactions with the chiral environment. For example, for transport through a large molecule, an electron will encounter, visit, and pass through many atoms. At each encounter where the electron orbits the nucleus, the spin-orbit interaction depends on the orbital orientation and will lead to some weak spin polarization. For a chiral molecule such as DNA the electron spin polarization is cumulatively enhanced by the preferred orbital orientations of the many surrounding atoms as it travels through the molecule, leading to the phenomenon of CISS.[12]

3.1   Simulations with Chiral Degrees of Freedom

The vast majority of theoretical CISS-related studies have relied on model Hamiltonian approaches, while conventional electronic structure methods, such as Density-Functional Theory (DFT) have yet to be fully implemented.[12,14,15,60] DFT-based spin-dependent transport calculations, within the Landauer approach and including spin-orbit coupling (SOC), have clearly demonstrated the influence of the helical geometry on the spin polarization[12,15] and they also correctly describe the increase of spin polarization with molecular length as observed experimentally.[16,61] However, the obtained spin polarizations are much smaller than the measured ones, suggesting that the theoretical description may be missing some key ingredients.

Recent experimental[12,62] and theoretical[63–65] results have suggested that electronic exchange interactions may play a fundamental role, eventually in combination with SOC.[65] In particular, exchange-related intermolecular interactions in arrays of helical molecules were shown to energetically stabilize a broken spin symmetry (singlet) state, the effect being absent in linear molecules.[7] As a consequence, a subsequent interaction with magnetized

surfaces can facilitate a symmetry breaking between enantiomers and lead to enantiomer discrimination, which would be mediated by exchange interactions. A further indication of the relevance of exchange contributions was found in:[64] a varying percentage of Hartree-Fock exchange contribution to exchange-correlation functionals strongly influences the size of the computed spin polarization in model helical molecular junctions.

Another interesting finding from[7] is the surprising ease with which formally closed-shell peptide helices can be spin-polarized in equilibrium when brought together in an array-like fashion, as opposed to isolated helices. The interaction with a metal surface was also found to be important. While past experience with DFT for spin-polarized molecules suggests some caution,[66] these results point to intermolecular interactions and interfaces being important for the first-principles description of CISS. Likewise, the role of the interface (possibly combined with the collective properties of molecular assemblies) for magnetic signatures in electron transport has been explored experimentally.[1,52,67] Beyond the description of exchange/electronic interactions, intermolecular and interface effects, it might be important to consider nuclear dynamics in addition to the electronic ones.[68–70] As a complement to these efforts establishing a comprehensive first-principles theory of CISS, chemical concepts extracted from first-principles calculations on helical molecules, such as electron transport pathways[14,52] and imaginary components of the Hamiltonian[64] may provide first steps towards understanding structure-property relationships in CISS.

In spite of the many attractive features of the description of CISS within a first principles framework, theoretical studies have primarily relied on model Hamiltonians, since *ab initio* calculations on complex helical structures can be challenging.[64,73] Most standard implementations of DFT can treat periodic and/or finite molecular systems, which can necessitate the inclusion of hundreds or even thousands of atoms in the simulation cell while studying such a structure. The computational time for ground state calculations using local or semi-local exchange correlation functionals scales cubically in the number of atoms in the simulation cell, while those employing Hartree-Fock or hybrid exchange scale as the fourth power. In
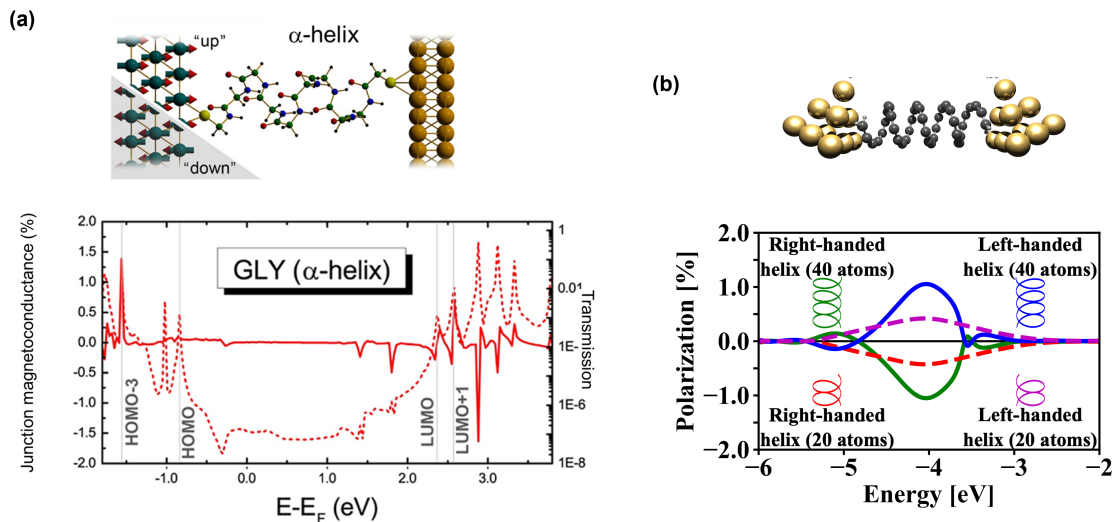
Fig. 7: (a) For a realistic peptide helix, a DFT-based Landauer approach including SOC yields spin polarization as rather narrow peaks far from the Fermi energy (solid line in the plot, reported as junction magnetoresistance; PBE).[71] (b) For a model helix of equidistant carbon atoms (capped by two hydrogens at each end), spin polarization over a broad energy range close to the Fermi energy is obtained, but it can be traced back to SOC transfer from the gold electrodes rather than resulting from SOC intrinsic to the helix (in the plot, the Fermi energy is between -5 eV and -4 eV for gold; B3LYP).[72] Note that the exchange-correlation functional PBE (plot in (a)) features 0% Hartree-Fock exchange, while B3LYP (used on the right) has 20%, and that the absolute values of spin polarization depend on this exchange admixture. Importantly, the polarization changes its sign when the helicity is inverted, and increases with molecular length (plot in (b)). Reprinted with permission from Refs. 71 and 72. Copyright 2018 and 2020 by the American Chemical Society.

view of this, systematic first principles simulation techniques which treat the helical symmetry exactly[74,75] (and therefore employ only a minimal unit cell to represent the system being studied) and efficient methods for computing exchange interactions[76,77] within such a symmetry adapted framework, are likely to emerge as powerful tools for DFT studies of the CISS effect in complex helical structures, in the near future.

The development of first-principles descriptions of molecular properties has been (and still is) profiting from quantitative benchmark experiments.[78] As is often the case in molecular electronics and spintronics, the lack of detailed atomistic control makes it extremely challenging to come up with such quantitative benchmark experiments for CISS. Therefore, it is crucial to have systematic experimental studies of the qualitative dependence of SP on

molecular structures and their arrangements, as recently provided in.[63] Together with further related studies, *e.g.*, on the role of local vs. axial chirality or on subtle structural modifications via chemical substituents or heteroatoms, this could provide a strong foundation on which further developments of a first-principles theory of CISS could build.

Finally, besides their relevance for the spin transport physics or for Heisenberg-type spin-spin interactions with magnetic substrates, helicity-dependent electronic exchange effects may lead to a reconsideration of standard expressions for induction and dispersion forces between chiral molecules. In fact, and similar to circular dichroism, both electric dipole and magnetic dipole contributions are required, allowing for chirality-sensitive forces[79,80] with potentially far-reaching consequences in, *e.g.*, the study of intermolecular interactions in biology. These considerations are summarized in the schematic in **Fig. 8**.

$$V(R) \overset{?}{\sim} -\frac{C_6}{R^6} \pm \frac{C_x^{helix}}{R^6}$$
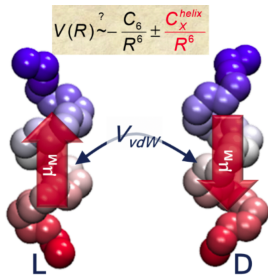
Fig. 8: In the case of chiral molecules, induction *and* dispersion forces encoding electric dipole-dipole interactions require additional modifications to account for exchange-mediated interactions related to the CISS effect.

The CISS effect observed in single peptide molecules with well-defined chirality (L- and D-peptides) was recently explained. The transport model was based on the Landauer regime and using the Green's function technique. In the presence of spin polarization effects, the conductance is spin-dependent and the transmission contains the information of the molecular chirality, helicity, and the propagation direction. This theoretical model was able to explain four possible scenarios of the observed current asymmetries in single chiral molecular junctions sandwiched between a polarized Ni tip and Au electrodes.[13] These four different scenarios with different conductance show that spin rectification application close to the zero-bias limit might be possible, and have opened the way for a new generation of molecular

23

devices based on spin filtering that can be used to probe novel ideas based on spintronics and spin-selectivity devices [9].
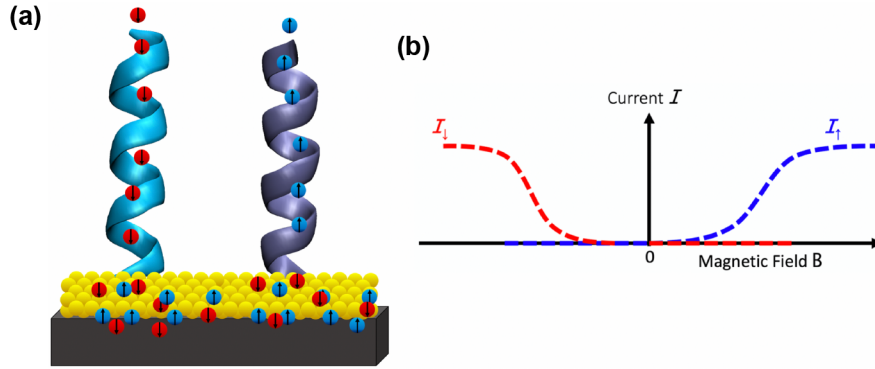
Fig. 9: **(a)** Functionalized gold substrates with individual peptide molecules with well defined chirality for spin selective nanodevices. **(b)** Application of CISS in spin rectifiers.

Starting from the Dirac Hamiltonian for a free electron, Kurian[81] has made an intriguing prediction in the non-relativistic limit due to a static magnetic field, for a quantum field-theoretic effect that is orders of magnitude larger than the quantum mechanical Zeeman shift. Such a discrepancy could be the source of the experimental gap in spin polarization described by current chirality-induced spin selectivity (CISS) theory. In the low-mass approximation for free electrons (where chirality coincides with helicity), Kurian derives a symmetry for such a system that is evocative of spin-to-orbital angular momentum (OAM) conversion demonstrated in vortex beams, but employing the expectation values for the energy and chirality shifts. This so-called chirality-energy conversion appears to arise from fundamental magnetic symmetries of free electrons under the influence of static fields, and such mutually correlated changes in energy and chirality can be directly measured in nano-, meso-, and macro-scale systems. A simple example of this sensitive dependence has been demonstrated in the chirality of nascent crystals and low-energy fluctuations introduced by perturbing the crystallization solution.[82]

Understanding the physical basis of CISS[64] continues to be a challenge. Nevertheless, minimal models for the spin-polarization mechanism has helped pave the way in exploring scenarios, first at a bare bones model scale to then follow by an analytical tight binding ap-

proach. These involve a first order approximation to the orbitals and couplings involved and then proceed to a detailed understanding including realistic features of the actual molecular structures involved. The history of theoretical approaches to CISS started trying to explain experiments of point chiral molecules in gas phase.[83,84] The theory recognized spin polarization as a single molecule effect where the spin-active coupling is the SOC between the scattered electron and the nuclear potential.[84] The theory based on symmetry considerations and geometry of the target-molecule system, agreed well with experiments[85] but it was a very small effect where polarization asymmetry was $\sim 10^{-4}$. It was then a tantalizing surprise when Ray *et al.*[12] reported a much larger effect in chiral self-assembled monolayers (SAMs) of aminoacids. Once more minimal models were proposed using the Born series.[15] A model of double scattering of single molecules, surmising a SO coupling arising from C, N, O atoms produced a chirality dependent polarization of a few percent. One of the most striking predictions of the theory was the existence of energy windows for the optimal action of the SO coupling[86] that was later corroborated by Rosenberg *et al.*[87] Additional more sensitive experiments on DNA SAMs[62] showed extraordinary electron polarizations leaving the theory underestimating the CISS effect by a factor of 10. No further improvements of the theory in this regime have taken place as far as we know. Further experimental progress[40] allowed for single molecule measurements, and simple tight-binding minimal models were proposed[16,88] assuming quantum coherence and a large SO coupling as an adjustable parameter to fit the large polarization reported experimentally. A further step to include geometrical arrangement of the orbitals and atomic source for the SO coupling was taken in,[89] using an analytical Slater-Koster approach that identified the transport SO coupling as a first order effect in the helical geometry. Such a spin-coupling goes to zero in non-chiral geometries and obey time reversal symmetry with eigenfunctions coming in Kramer pairs.[90] An important ingredient of the minimal model was to include the problem of the electron bearing orbital filling in determining the energy dispersion of the model. The mechanism for spin-polarization in the presence of bias is connected to the fact that time-reversal symmetry is broken and a spin

direction is preferred corresponding to one of the helicity eigenstates of the Hamiltonian.[86,89]

The minimal model for DNA with details of the relation between geometry and transport eigenstates has recently led to a proposal to use mechanical deformations in order to assess the orbital involvement in spin transport[91] and test models.

It seems to be clear that the SO coupling is the spin-active ingredient[86] for the molecular length-dependent spin polarization process. Minimal models place the strength of this coupling, of atomic origin, in the range of 1-10 meV[89] and may be modulated by orbital overlap effects[89,92] and hydrogen bonding as an additional source of the electric field scaling-up the effective SO coupling, particularly for biological molecules, *e.g.*, DNA and polypeptides.[93] A major consideration that the future models must contemplate is that the two main mechanisms involved in charge transport in chiral biological molecules and polymers are tunneling and hopping.[94,95] Which mechanism dominates transport depends on Peierls-like instabilities and heterogeneities intrinsic to the molecule and the environment where the molecule dwells.[96] A simple model for almost filled electron bearing orbitals showed a promising mechanism for CISS based on spin-selective transmission under a barrier,[97] as shown in **Fig. 10**. The mechanism is based on the torque coupled interplay between electron spin and molecular angular momentum. Both mechanisms, tunneling and hopping, could be strongly influenced by spin polarization modifying the effective length of electron transfer. In any event, the CISS mechanism should be considered in the context of both transport mechanisms.

Coupled to the transport mechanism, all the models proposed to explain CISS have focused on processes involving quantum coherent aspects, non-unitary proposals have been contemplated.[98] CISS occurs at room temperature so, how do these quantum mechanisms survive? Generic voltage-probe leakage is a minimal model to foresee decoherent effects. In fact, such probes have shown to be a route to spin-polarization as a breaking of time reversal symmetry would imply. A more explicit model for decoherence would be to include the electron-phonon coupling as a major mechanism for decoherence[98,99] and describe how electronic and spin degrees of freedom couple to the phonon bath in the tunneling process. A

first analysis has revealed a partial electron-phonon decoupling to first order in longitudinal modes[100] while the coupling persists for optical modes in DNA. This mechanism could also operate in oligopeptides. All the theoretical and computational tools associated with this approach are ready to assess the influence of spin-phonon coupling in electron transfer and transport in chiral molecules.
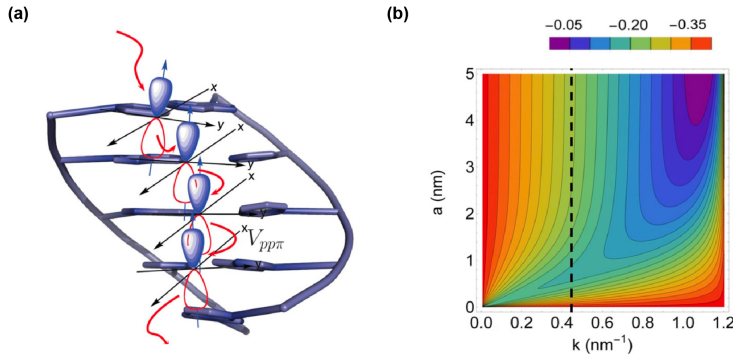
Fig. 10: Spin-orbit interaction and spin selectivity for tunneling electron transfer in DNA. **(a)** Schematic of DNA molecule with orbitals for electron transport. The p_z orbitals are perpendicular to the baseplanes and coupled by $V_{pp\pi}$ Slater-Koster matrix elements. **(b)** Plot of spin asymmetry P_z as a function of scattering barrier length a and input momentum k. Adapted with permission from Ref. 97. Copyright 2020 by the American Physical Society.

4 Engineered Chiral Materials

4.1 Influence of the Substrate Spin-Orbit Interaction on Experimental Spin Polarization and Chiral-Induced Spin Selectivity

Early experiments on CISS were performed mostly on gold substrates because the helical biomolecules studied could at one end easily be thiolized and then form a strong bond with the substrate. Heavy metal substrates like gold are known to emit electrons with a preferential spin orientation when excited by circularly polarized light. Their spin orientation

is linked to the helicity of the light. In noble metals the d-electron spin-orbit coupling constant increases from 0.1 eV to 0.25 eV, and 0.72 eV, for Cu to Au, respectively.[101] On single crystal Au(111), circularly polarized radiation in the ultraviolet range just above the work function excites electrons in the $\Lambda_6^1 \leftarrow \Lambda_4^3 \Lambda_5^3$ transition, from the spin polarized occupied band into an unoccupied plane wave final band (Λ_6^1) near the L point of the Brillouin zone. For Cu and Ag, however, besides an already lower spin-orbit coupling, the initial state is a Λ_6^3 state which produces only a very weak spin polarization.[101] Such an excitation with circularly polarized light then yields longitudinally polarized electrons with respect to the quantization axis being the k vector of the exciting radiation. It is thus important to excite the system under normal incidence and also extract the electrons normal to the surface. For Au(111), spin polarization values up to $P = 30\%$ are obtained just above the vacuum level.[62,101] Due to the electronic structure of polycrystalline gold the spin direction is reversed compared to Au(111), and also the absolute value is significantly smaller. Nevertheless, this substrate behavior spurred the idea that the strong spin-orbit interaction in heavy metals reaches out to the helical adsorbates made out of light atoms, like C, N, O, and H.[102]

For these three noble metals systematic experiments on CISS were performed for adsorbed monolayers of enantiopure hepta-helicene.[103] For linearly polarized excitation light which produces unpolarized photoelectrons in the substrate, M-helicene yields on Cu(332) a spin polarization of $P = -6.7\%$, on Ag(110) one of $P = -9.0\%$, and for Au(111) of $P = -8.0\%$, see **Fig. 11** center (blue) histograms. Circularly polarized excitation, which already produces polarized photoelectrons in Au and to a limited extend also in Ag substrates, results in the generation of an additional spin polarization. This is in particular noticeable for Au(111). There, clockwise (cw) circularly polarized light (upper green histograms) yields a total spin polarization of $P = -35\%$ for M-[7]-helicene, while counter clockwise (ccw) polarized light (lower red histograms) produces only $P = -22\%$. For P-helicene the sign of the spin polarization switches, and also the action of cw and ccw polarized light on the total spin polarization is reversed.[103]
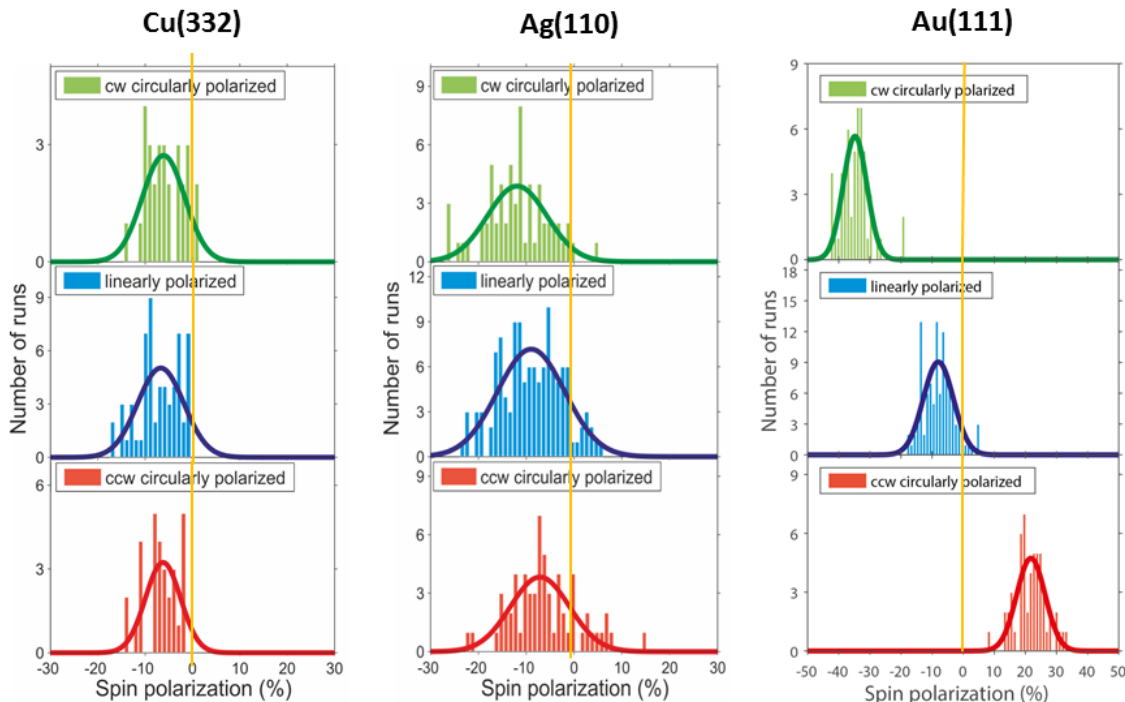
Fig. 11: Spin polarization of photoelectrons from Cu, Ag, Au substrates transmitted through a monolayer of M hepta-helicene. Green, blue, and red histograms (from top to bottom) represent excitation by clockwise (cw) circularly, linearly, and counter clockwise (ccw) circularly polarized light at $\lambda = 213$ nm, and thus emitting electrons slightly above the vacuum level of the systems.

Earlier it was already shown that the CISS effect occurred for bacteriorhodopsin adsorbed on aluminum oxide[104] and for DNA bound to Si(111),[105] both lacking significant spin-orbit coupling. The action of the helical organic molecules on CISS is thus independent of the substrate, however, an initial spin orientation may be beneficial in reaching high spin polarization. It is thus a promising result that neither heavy substrate elements nor magnetic substrates are required to generate spin polarized electrons from helical organic molecules. This lifts possible restrictions in designing spintronic elements, as gralizes the application of CISS into (electro-)chemistry[66] and to bio systems.[104]

4.2 Heavy-Element Insertion

Early investigations of spin-dependent attenuation of electron beams through vapor-phase

chiral molecules by Mayer and Kessler indicated that the presence of a heavy element, such a ytterbium, bound to the chiral molecule, could dramatically enhance the transmission asymmetry observed.[106] These findings agree qualitatively with earlier theoretical models indicating that the presence of a heavy atom in a chiral molecular environment should enhance the spin- and chirality-dependent asymmetry in electron-molecule interactions, likely due to increased spin-orbit coupling effects.[84] These results were further expanded using chiral bromocamphor derivatives.[107]Subsequent experiments demonstrated that the degree of spin-polarized electron transmission asymmetry could be modified for nearly identical molecules simply by substituting the coordinating species. Spin-selective electron transmission asymmetry through vapors of chiral camphor derivatives was observed to increase roughly along with the atomic number of the coordinated atom, as Pr (Z = 59) < Eu (Z = 63) $\sim$ Er (Z = 68) < Yb (Z = 70).[108] Interestingly, molecules with multiple heavy inclusions, such as dibromocamphor, did not exhibit higher asymmetries than their singly brominated counterparts. These trends are further supported by recent experiments carried out on single-stranded DNA SAMs designed to form DNA hairpins and specifically coordinate Hg^{2+} ions at thymine-thymine mismatch sites.[49]

Employing ultraviolet photoelectron spectroscopy to characterize magnetization-dependent ionization energies of DNA SAMs formed on ferromagnetic substrates, Stemer *et al.* (see **Fig. 12**) reported that the incorporation of a single equivalent of Hg^{2+} into DNA hairpins constituting only a single helical turn is sufficient for the manifestation of spin-dependent effects at room temperature. No magnetization-dependent effects are apparent in the samples composed of identical DNA sans Hg^{2+}. At high degrees of metal loading, the tertiary structure of the DNA hairpins was found to invert. This inversion was accompanied by a complementary reversal in the preferred magnetization orientation for photoionization. Analogous to earlier experiments by Kessler and Mayer,[106] increased incorporation of heavy constituents did not appear to further increase spin-dependent interaction asymmetries, indicating that multiple heavy inclusions may induce compensating instead of amplifying effects.
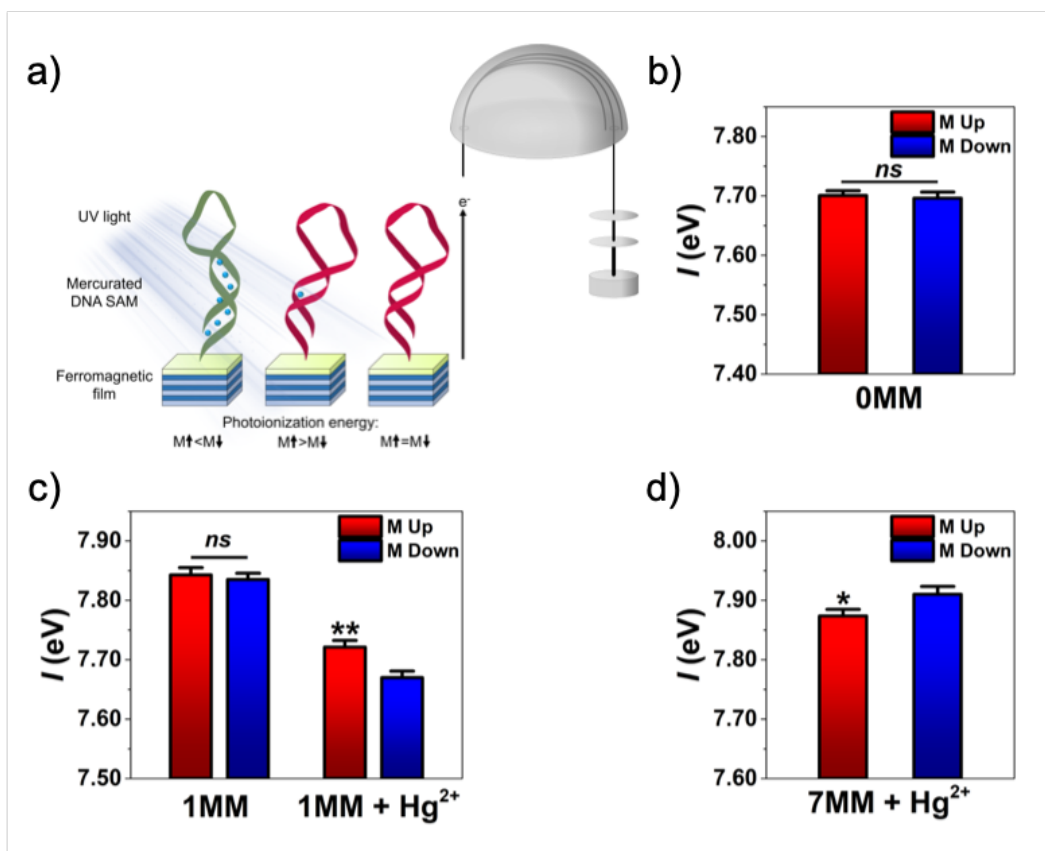
Fig. 12: (a) Schematic depicting spin-dependent photoelectron scattering through self-assembled monolayers of DNA hairpins on ferromagnetic films, characterized by ultraviolet photoelectron spectroscopy. Spin-dependent ionization cross sections result in differential charging, physically manifested as substrate magnetization-dependent photoionization energies of the chiral organic films. **(b,c)** Spin selective effects were only observed in short (~ 1 helical turn) DNA hairpins that contained mercury bound at thymine-thymine mismatches (MM) due to enhanced molecular spin-orbit coupling. **(d)** Spin selectivity was reversed in DNA hairpins containing 7 MM and stoichiometric amounts of mercury ions, which was shown to invert the chirality of the helical hairpins. Reproduced with permission from Ref. 49. Copyright 2020 by the American Chemical Society.

These studies highlight to direct tunability of chiral molecular systems via the incorporation of heavy species, a powerful tool in engineering highly spin asymmetric systems for spintronics and quantum computing applications.

5 Chirality in Biology

Chirality plays a fundamental role in a host of physical processes, ranging across vast

orders of magnitude in scale and including all biological interactions. Researchers have pondered the origins of this universal handedness from multiple vantage points, including cosmological,[109] astronomical,[110] astrophysical,[111] biomolecular,[1,81,112] and quantum field-theoretic.[81] The connection between spontaneous symmetry-breaking, chiral effects, and life is therefore an intimate one, but this nexus has not been easily understood, considering the diverse theoretical and experimental tools needed to probe the phenomena.

Such sensitive relationships between the chirality of underlying quantum (charge, spin, exciton, plasmon) states and biological function abound. Co-author Kurian and colleagues[113] have shown that certain chiral enzyme complexes with palindromic symmetry conserve parity, and that the chirality is essential for the global synchronization of plasmon-like van der Waals fluctuations and for the symmetric recruitment of energy from DNA substrates for the formation of double-strand breaks in a site-specific fashion. The application of tools from quantum optics to describe biological chromophore lattices has resulted in the recent prediction of ultraviolet superradiance in certain cytoskeletal filaments,[113] which exhibit a stark spiral-cylindrical chiral symmetry (**Fig. 13**) that is reflected in the excitonic wave-function distributed over the chromophore network (**Fig. 14**). The relationship between this electronic superradiance and its spintronic counterpart is an active area of investigation, which may be exploited for advanced biosensors and diagnostics.

Exploiting the CISS effect for prediction, control, and enhancement of biological response is a tantalizing possibility. Take, for example, the case of human immunity, which is of particular interest in the midst of the COVID-19 pandemic: T-cells initiate the body's adaptive immune response by interacting, via their T-cell receptors, with major histocompatibility complex (MHC) peptides on antigen-presenting cells that have been exposed to pathogens. MHC molecules are membrane-bound glycoproteins that form unusually stable bound configurations with antigenic peptide ligands (pMHC), displaying them on the cell surface for recognition by T-cells via T-cell receptor (TCR) engagement.[116] TCR activation promotes several signaling cascades that ultimately determine cell fate by regulating cytokine pro-
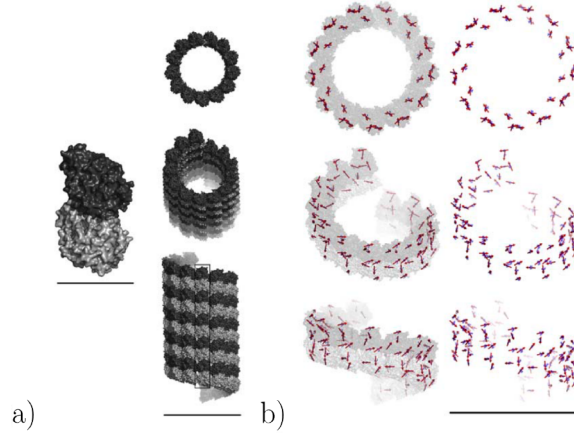
Fig. 13: (a) Tubulin proteins with scale bar 5 nm (far left) polymerize into microtubules with scale bar 25 nm (left) with (b) highly ordered arrays of tryptophan amino acids (right and far right) that absorb radiation in the ultraviolet spectrum. Reproduced with permission from Ref. 114. Copyright 2019 by IOP Publishing Ltd.
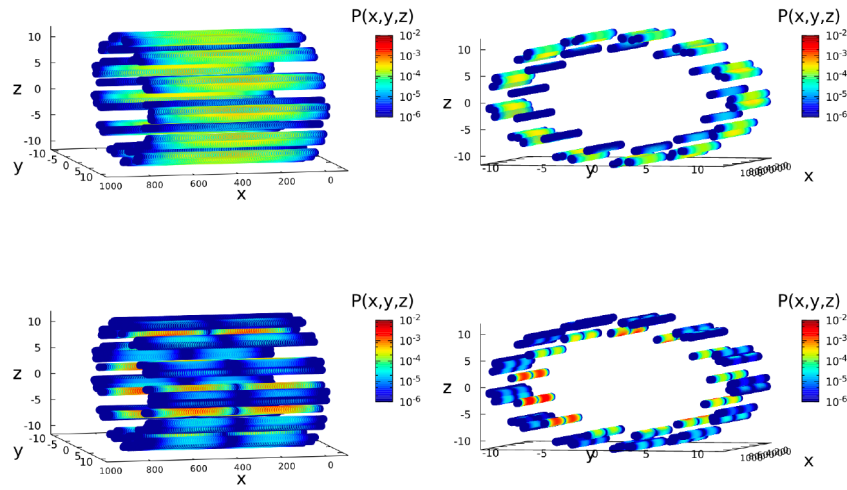
Fig. 14: The quantum probability of finding the exciton on a tryptophan of a microtubule segment of 100 spirals with 10,400 tryptophan molecules, is shown for the extended super-radiant state in lateral view (top) and in cross section (bottom). Lengths are expressed in nm. Reproduced from with permission from Ref. 114. Copyright 2019 by IOP Publishing Ltd.

duction, as well as cell survival, proliferation, and differentiation.[117] Studies have found that spin-polarized states of antigenic peptides may affect the ability of a TCR to recognize different peptides by virtue of conformationally-induced spin moments, rather than sheer topology-based affinity, a condition that would render the immune recognition process as fundamentally spin-specific.[115,118] In the work by Antipas *et al.*,[115] different pMHCs with
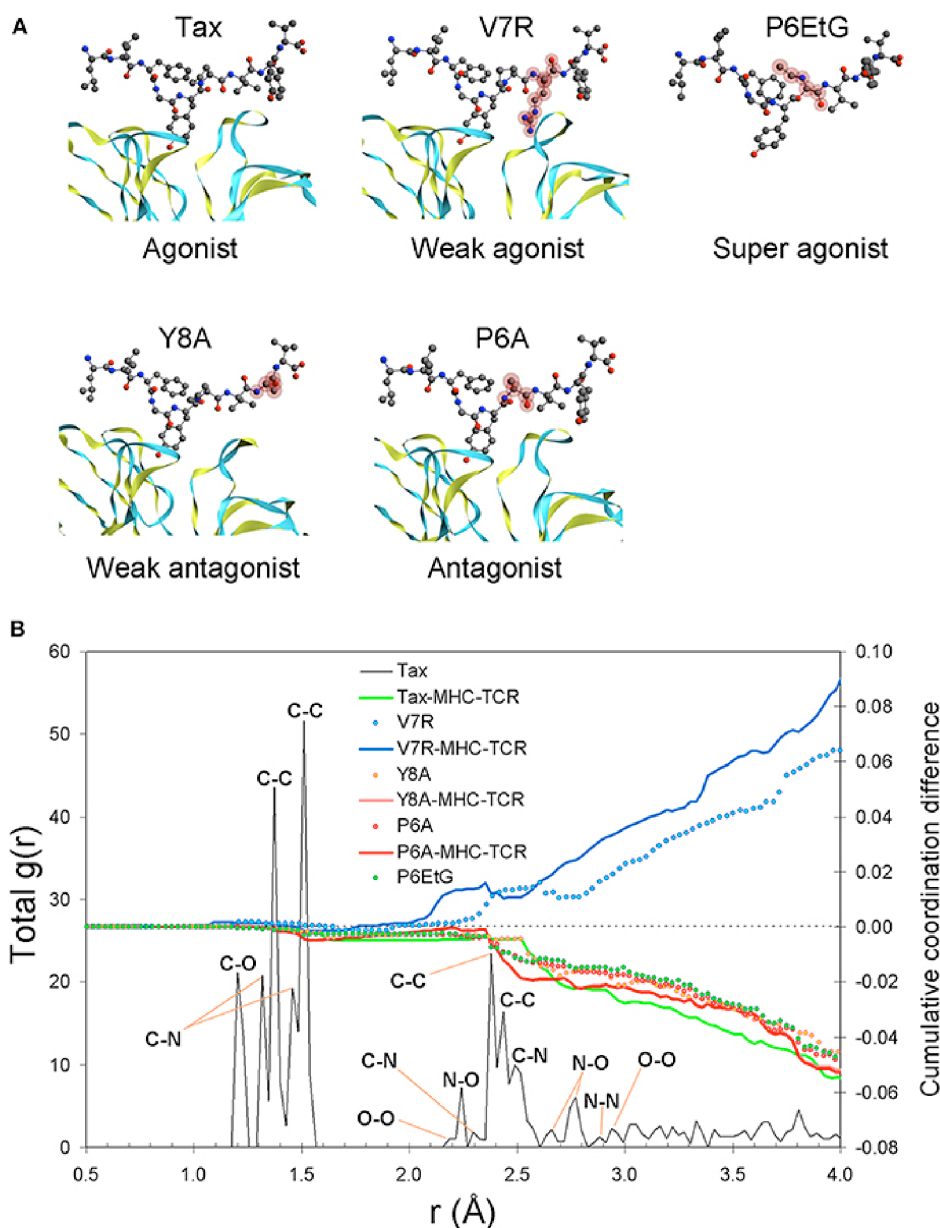
Fig. 15: **(A)** Different peptide structures that are unprotonated. **(B)** The pair distribution function (PDF) is shown for the different peptides in (A) as a function of interatomic distance r. Reproduced with permission from Ref. 115. Copyright 2015 by Frontiers Media SA.

near-identical stereochemistries were complexed with the same TCR, resulting in induced distinctly different quantum chemical behaviors that depended on the peptide's electron spin density and expressed by the protonation state of the peptide's N-terminus (**Fig. 15**). Spin-polarization of different peptides can thus be correlated to downstream signal transduction pathways and their activations of biosynthesis at the transcriptional level. Other studies

have shown that noncovalent and dispersive interactions between biological molecules are key for their functions, in which the electronic charge redistribution in chiral molecules is accompanied by spin polarization.[1,119] Studying chirality, spin polarization, and downstream response in pMHC-TCR interactions could therefore help to improve our understanding of the impact of chiral-quantum effects on the human immune response, and to develop better tools for therapeutic intervention.

6 Chiral Degrees of Freedom in the Interaction of Matter and Electromagnetic Fields

6.1 Chirality Imprinting

Handedness, or chirality, may be transferred from a chiral object to an achiral object or achiral medium, *i.e.*, chiral molecules adsorbed on surfaces induce chirality on the substrate. Indeed, we have found in our theoretical analysis that that CD and optical rotatory dispersion signatures can be induced through chiral imprinting.[120–122] In fact, it is possible for the magnitude of the imprinted chiro-optical signature to be larger than that of the chiral 'die' itself.

A kind of handedness can be imparted to excited states using circular polarized excitation. For example, molecules with degenerate x- and y- polarized excited states, when excited by left- vs. right-circularly polarized light are complex conjugates of one another (*i.e.*, $\Psi_+ = \Psi_-^*$). If the excited state induces chemistry on a time scale that is fast compared to the time scale of decoherence, the chemistry may be imprinted by the handedness of the light excitation. For example, Skourtis[123] has predicted that electron transfer yields may be influenced by the handedness of circular excitation. Combining circularly polarized excitation with chiral bridges can thus produce novel effects on electron transfer chemistry as well.[124,125]

6.2 Exploring Photonic Chirality through Orbital Angular Momentum

Photon packets can be described by several quantum numbers that describe their intrinsic spin angular momentum (SAM) their number state, their energy, and their transverse spatial mode. For spin and transverse modes the light can carry angular momentum which can interact both classically and quantum mechanically with a material. While SAM is widely used for QIP protocols,[126] helical transverse chirality (orbital angular momentum, or OAM) is not commonly used to transmit or encode additional information in the emitted photon stream from a material.[127]

Similarly to SAM, OAM modes carry quantized angular momentum in proportion to the electric field phase difference around a centrosymmetric position. OAM can thus carry quantum information through pure and entangled states.[128] One exciting potential applications of OAM will be the ability to drive transitions beyond dipole limit.[129] Many qubit transitions are defined within a quadripolar or magnetic dipole subspace and such transitions can only be driven by electric field gradients, carried in the OAM field. Improving the fidelity of OAM quantum information transfer may require near-field OAM photonics, in visible and microwave regimes.[130,131]

Recently researchers have demonstrated that OAM can induce specific quantized transitions, in an atomic ions,[132] highly bound Rydberg excitons in semiconductors[133] and potentially in non-degenerate valley states of 2D material OAM to drive statespotential for helics.[134] These experiments demonstrate the potential for helical OAM to drive states amenable for quantum information, and given the two latter cases, extended chiral excitons may be the key to unlocking the potential of chiral transverse modes in information transduction.

7 Chirality in the Quantum Sciences

A scientific revolution is underway enabled by quantum information processing (QIP). Successful quantum hardware will depend both on incremental technological improvements and on disruptive applications of physical laws underpinning how qubits read, store, and transduce information. The challenge addressed here is to rethink quantum information protocols to incorporate chiral 'handles': can nanoscale chirality be leveraged to create innovative approaches to QIP?

Using chirality as a design basis for quantum devices is unprecedented, *i.e.*, aiming to control spin, charge, and energy transport through molecules and interfaces so that quantum information can be preserved and transferred at room temperature. A key concept is the manipulation of the magnetic response in chiral molecules and engineered nanomaterials, especially via the recently discovered CISS effect. This approach includes controlling the spin filtering and polarization capabilities of molecules and engineered nanomaterials, and generating qubits through molecular design, surface architectures, and tailored interactions with light with chiral degrees of freedom. A complementary focus is the study of quantum transduction processes at soft-hard material interfaces, involving both the transfer of spin polarization from electrons to nuclei and field-mediated chirality transfer.

7.1 Spin Superradiance and Chiral-Induced Spin Selectivity

Cooperative effects arise from collective behavior of the constituents of a system, and therefore they are associated with the system as a whole and not to its individual components. These phenomena occur at every scale, ranging from the structure of atoms in crystals to ferromagnetism, superradiance (SR) and superconductivity, functionality in complex molecules and the emergence of life from biomolecules.[135]

One of the most interesting properties of cooperative effects is their robustness to the noise induced by external environments. For this reason, cooperative effects could play an

essential role in the successful development of scalable quantum devices able to operate at room-temperature.

A well-known example of robust cooperative effect is superconductivity, but other quantum cooperative effects, such as SR, have also been shown to be robust to noise.[136,137] For instance, in the case of SR, the coupling of an ensemble of emitters to an external field can induce an energy gap; this makes superradiant states robust to disorder. Interestingly, the superradiant energy gap, in certain limiting cases, is the same as the superconducting gap.[138] SR, first proposed by Dicke in 1954,[139] arises from the excitation of an ensemble of individual two-level systems and results in an emissive, macroscopic quantum state. Superradiant emission is characterized by an accelerated radiative decay time, where the exponential decay time of spontaneous emission from the uncoupled two-level system is shortened by the number of coupled emitters. In addition, when the excitation is incoherent,[140] SR exhibits a delay or build-up time during which the emitters couple and phase-synchronize to each other, and which corresponds to the time delay between the excitation and onset of the cooperative emission.

SR has been observed in a variety of systems,[141] with some of the most recent examples being cold atomic clouds,[142] photosynthetic antenna complexes,[143] molecular aggregates,[144,145] quantum dots,[146,147] nitrogen vacancies in nanodiamonds,[148] and lead halide perovskite nanocrystal superlattices.[149] This effect is relevant in enhancing absorption and energy transfer, which has been proposed to improve the efficiency of light-harvesting systems and photon sensors.[150–154] SR also leads to spectrally ultranarrow laser beams.[155]

Even if the vast majority systems exhibiting superradiance involve electronic transition at optical frequencies, SR has also been observed in spin systems.[156] Spin SR have attracted much attention recently due to its many possible applications to sensing and spin masers.[157–160] In particular, systems exhibiting spin superradiance could be used to produce sensitive detectors. Spin SR can be triggered by extremely weak external pulses; given that the delay time is exponentially dependent on the intensity of the external pulse, measuring

the delay time of a superradiant burst provides an accurate evaluation of the triggering intensity. Another very interesting application of spin SR is spin masers.[161–163] A superradiant spin system is a source of coherent radiation at radiofrequencies, analogous to lasers operating at optical frequencies. The maser, with a frequency 0.3–300 GHz and a wavelength between 1 m and 1 mm, is the microwave analogue of lasers, having several important applications, *e.g.*, in ultrasensitive magnetic resonance spectroscopy, astronomy observation, space communication, radar and high-precision clocks.

The key to spin SR and spin maser is the population inversion of the emitters. In spin systems, population inversion corresponds to spin polarization – which is a precondition for SR emission and Maser operation when a polarized spin population is present in a microwave resonator cavity. For this reason it would be very interesting to exploit the CISS effect[72,164] in connection with spin SR and spin masers. Indeed, the spin-polarized beam emerging from chiral molecules due to the CISS effect could be used to induce a SR pulse. SR could thus help elucidate the CISS effect. A beam of polarized electron spins could be also used to operate a spin maser when coupled to a microwave resonator cavity. Moreover, it is known that a polarized electron beam couples with nuclear spins by hyperfine spin-spin interactions. This coupling would produce a shift of the NMR frequency of nuclear spins and would thus be able to enhance the coupling between the nuclear spins and the resonator. These effects could be used both to study the CISS effect and to build more efficient SR or Maser nuclear spin systems.

7.2 Controlling Spin Polarization and Entanglement in a Hybrid Chiral Molecule/ Quantum Dot System

To understand CISS has remained a theoretical challenge. A recent study[165] revealed that the CISS effect vanishes when all electron states with the same energy are equally likely – a consequence of the Onsager reciprocal principle. The generality of this result means that the CISS effect needs to be understood in terms of the specific experimental settings.

Three possible situations were pointed out:[165] the electronic states with the same energy not being equally probable (*e.g.*, for electrons generated optically by a laser), the presence of accidental degeneracy in the molecular spectrum which enhances the spin-orbit coupling, or a magnetic lead. More recently, an analysis based on symmetry in electronic transmission was carried out to gain insights into the origin of CISS.[72]
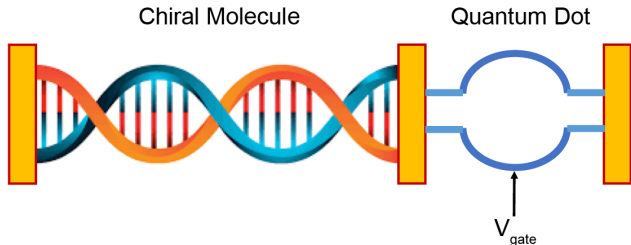
Fig. 16: A schematic illustration of a 'super chiral molecule' – a coupled chiral-molecule/quantum-dot hybrid structure, for controlling and manipulating spin polarization and entanglement. The gate voltage is applied to change the quantum dot structure for controlling spin polarization.

While strengthening the spin-orbit coupling through, *e.g.*, coupling a chiral molecule to a heavy metal or a superconductor can enhance spin polarization, control and manipulation are difficult. A potential approach is to exploit a hybrid structure that couples a chiral molecule with a two-dimensional (2D) quantum dot to form a 'super chiral molecule' for controlling and manipulating spin polarization, as schematically illustrated in **Fig. 16**. The idea is originated from the recent work by some of the authors on controlling spin polarization by exploiting classical chaotic dynamics[166,167] and spin Fano resonances.[168]

Intuitively, the role of classical dynamics in spin transport is intriguing from the point of view of classical-quantum correspondence, as spin is a purely relativistic quantum mechanical variable with no classical counterpart. Nevertheless, due to spin-orbit coupling and because the orbital motion does have a classical correspondence, the nature of the classical dynamics can affect spin. Full quantum calculations and a semiclassical theory revealed[168] that the spin polarization can be effectively modulated if the geometrical shape of the quantum dot structure can be modified to produce characteristically distinct classical behaviors ranging

from integrable dynamics to chaos. Especially, chaos can play orthogonal roles in affecting spin polarization, depending on the relative strength of the spin-orbit coupling. For weak coupling with a characteristic interaction length much larger than the system size, chaos can preserve and even enhance spin polarization. In the strong coupling regime where the interaction length is smaller than the system dimension, chaos typically deteriorates or even destroys spin polarization. For 2D materials such as graphene, a quantum dot and its geometric shape can be realized by applying a properly designed gate potential. The total spin polarization from the hybrid structure can then be manipulated electrically.

In electronic transport through mesoscopic systems, the various resonances associated with physical quantities such as conductance and scattering cross sections are characterized by the universal Fano formula.[169] Quite recently, a Fano formula was discovered[168] to characterize the resonances associated with two fundamental quantities underlying spin transport: spin-resolved transmission and the spin polarization vector. In particular, the Green's function formalism was generalized to spin transport and the Fisher-Lee relation was employed to obtain the spin-resolved transmission matrix, enabling the spin polarization vector to be calculated and leading to a universal Fano formula for spin resonances. A phenomenon with implications to control and manipulation is that the resonance width depends on the nature of the classical dynamics as defined by the geometric shape of the dot. Since characteristically distinct types of classical dynamics including chaos can be readily generated in the quantum dot through geometric deformations,[170] Fano spin resonances can be modulated accordingly. This provides a theoretical foundation for the general principle of controlling spin polarization in the super chiral molecule system through manipulating the classical dynamics in the quantum dot, which can be experimentally realized by applying a properly designed local gate potential profile. Likewise, modulating the classical dynamics in a different way can enhance the spin Fano resonance. The control principle was computationally demonstrated[171] in a key component in spintronics: a class of nanoelectronic switches, where the spin orientation of the electrons associated with the output current can be controlled

through weakening or enhancing a Fano resonance.

7.3 Quantum Information Storage and Transduction

We believe it is strategic and timely to exploit the distinctive properties of chiral molecules and chiral material interfaces for developing new room-temperature device technologies in quantum sensing, quantum storage and quantum computing.

Thus, tailoring orbital angular momentum couplings by acting either on the spin quantum states acting as qubits and/or on the interaction potentials opens up tantalizing possibilities for room-temperature transduction of quantum information.

Quantum information processing and quantum sensing have made enormous strides in the past couple of decades. Superconducting circuits and ion traps have led to a race for supremacy in quantum computing, whereas ultracold atoms and molecules, NV and other color centers have enabled a variety of approaches to quantum sensing (*e.g.*, magnetometry, dark-matter detection, atomic clocks). With the exceptions of NV centers and atomic vapors, these approaches require extremely low temperatures (mK range) to protect the coherent states and to allow sufficient time for entanglement to evolve, or measurements to be made. This constraint restricts their installation to locations with sizable infrastructure support. Currently, the main drawback of qubits based on defect centers is the difficulty of fabricating them at specific locations, selectively addressing different centers, and of establishing quantum information transfer beyond the short dipole-dipole interaction length scales.

In striking contrast to the approaches described above, chemical synthesis of chiral materials affords the opportunity to build novel quantum information systems from the bottom up, taking full advantage of the quantum properties of matter on the atomic scale. Chiral molecular systems differ from current qubit implementations described above in three important ways. First, chemical synthesis allows control over the nature of the qubit itself, thus enabling careful tuning of individual quantum states. Second, covalent and non-covalent interactions between molecules can be used to construct atomically precise arrays of qubits.

This approach offers the possibility of controlling and interrogating the properties of a qubit both in isolation and as part of an array, providing new insights into the quantum properties of multi-qubit arrays. Third, chiral molecules have the potential to serve as long-range quantum information transducers.

It may be possible to transfer chiral spin information between electrons and nuclei via hyperfine interactions, *e.g.*, from within topological insulators to DNA photolyase radical pair reactions at high temperature. Spin-polarized electrons can be generated on the surface of topological insulators (TI) through the application of an electrical current.[172] The coupling of the electron spin to the nuclear spin via hyperfine interactions highlights the ability to produce dynamic nuclear polarization (DNP).[172,173] A promising application is a rechargeable spin battery,[172] which could be used as ancillary qubits. From these recent results emerge two applications: **(1)** TIs can be used to generate spin-polarized electrons, which can interact with nearby DNA molecules and biomolecular structures through highly reproducible, high-precision contacts; **(2)** Interactions with radical pair states are also possible, particularly in the context of repair of lesions in duplex DNA, where the repair yield is dependent on the strength and angle of the applied magnetic field.[174] Chiral spin modes on the surface of a TI[175] can be used as an additional degree of freedom for manipulating the polarization.

Chiral molecules could also be harnessed for quantum information transduction. Nanochiral materials could be used as quantum wires connecting a node of quantum sensors. For example, we envision testing chiral materials as tractable, in chip solid-state quantum wires connecting established quantum sensors (*e.g.*, color centers in diamond, silicon or silicon carbide), see **Fig. 17**. Proposals for connectivity among quantum sensors has traditionally relied on dipole-coupled spin buses,[176] which unfavorably limit the maximal distance in between nodes, and which can hardly be engineered. Conversely, quantum information transduction through chiral materials will overcome both these limitations, and have already been shown to be capable of quantum information transduction and topological-like transport over longer distances and in complex environments.[62]
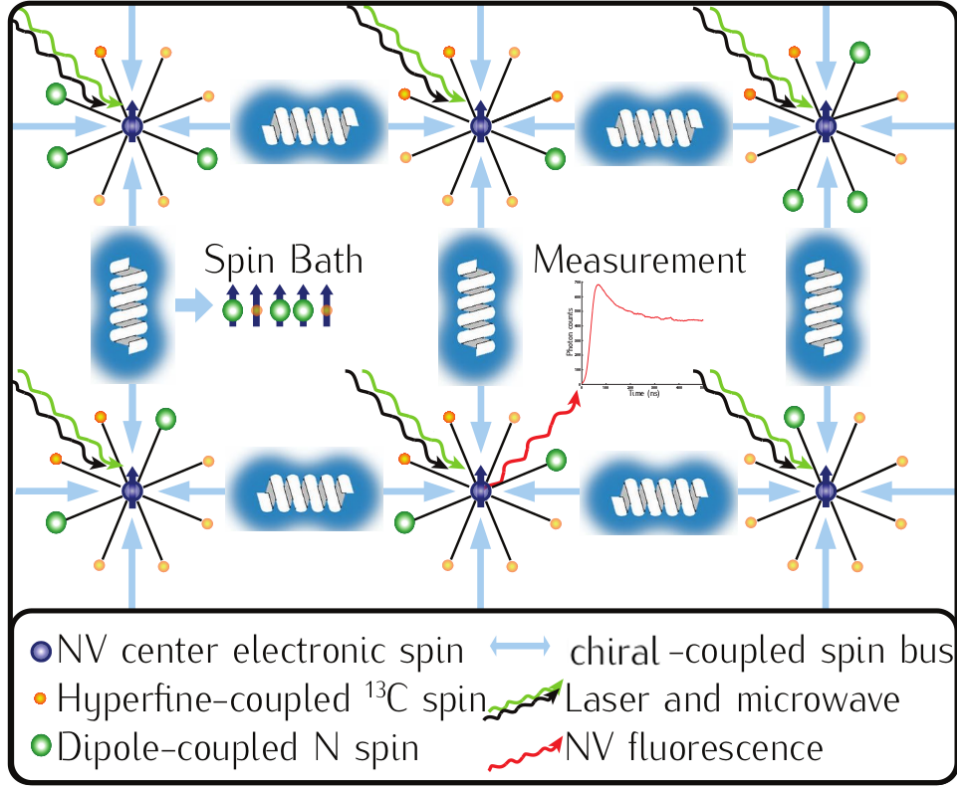
Fig. 17: Chiral molecules could be used as interconnects or quantum information transducers that have a longer-range than dipolar-coupled spin buses.

7.4 Decoherence and Entanglement Considerations

An important question for near room-temperature CISS-based quantum information is a good understanding of the decohering bath. Investigation of single-qubit coherence properties under controlled noise (electron-electron, electron-phonon scattering) environments will be needed to inform the design of novel chiral materials and devices for quantum information processing. For example, spin textures[177] are a complex result of electronic correlations. If electron-electron interactions can be effectively decoupled, CISS can still be sustained by the material, since it results essentially from the spin-orbit coupling and the breaking of inversion symmetry under electron transfer, transport or polarization conditions. Under-standing bath dynamics and application of reservoir engineering principles can be achieved with proof-of-principle experiments relying on controlled charge injection into nanochiral materials, combined with quantum information/sensing protocols for spin-state prepara-

44

tion/control/readout.

Another key issue is entanglement. For a quantum system with multiple degrees of freedom or subspaces, loss of coherence in a certain subspace is intimately related to the enhancement of entanglement between this subspace and another one. It would be useful to investigate intra-particle entanglement between spin and orbital degrees of freedom in the super chiral molecule system with different types of classical dynamics in the quantum dot. Of particular interest is the spin degree of freedom in the weak spinorbit coupling regime where, as existing studies suggested, [166–168] it is possible to use classical chaos to significantly enhance spin-orbit entanglement at the expense of spin coherence.

7.5   Control of Light-Matter Interactions

In addition, taken together, orbital and spin angular momenta provide exciting avenues for quantum control. The critical challenge for using OAM for quantum control is in enforcing the interaction of the emitter with the inhomogeneous spatial mode of the electromagnetic field, which is addressed by the following two questions:

(i) How can one design materials that interact strongly with orbital angular momentum fields via extended excitonic states? Many delocalized systems already strongly couple to spin AM through either macroscopic helicity (*e.g.*, helical molecular aggregates) or through degenerate points in their band structure (*e.g.*, valleytronic 2D materials), but spin AM combined with orbital AM remains experimentally underexplored. It needs to be established how mesoscopic helicity in novel designed and self-assembled materials can control and enhance interactions with orbital AM fields.

(ii) How can one implement sub-wavelength optical fields with orbital angular momentum that will strongly interact with matter? Near-field photonics can create field gradients that are far stronger than the free-space modes (thus preventing decoherence) and that can be used to drive high-order transitions (such as electric quadrupole) far more efficiently than the vacuum (*i.e.*, spontaneous emission). Controlling quantum information via spatially

engineered electromagnetic fields that provide environmental control of angular momentum would be transformative for quantum-enabled technologies.

8 Conclusion

In this extensive review, we have presented diverse systems in which chemical, materials, and electromagnetic chiral degrees of freedom could be harnessed for QIP. Collectively, this work aims to establish the field of chiral-enhanced QIP. Moving forward, chiral-enhanced QIP will require a multidisciplinary effort combining cutting-edge materials design and characterization with diverse theoretical methods, with long-term goal is to design and control chiral qubit spin states operating at room-temperature. We firmly believe that a chirality-based quantum leap will guide the next revolution in quantum devices.

References

1. Kumar, A.; Capua, E.; Kesharwani, M. K.; Martin, J. M. L.; Sitbon, E.; Waldeck, D. H.; Naaman, R. Chirality-induced spin polarization places symmetry constraints on biomolecular interactions. *Proceedings of the National Academy of Sciences* **2017**, *114*, 2474–2478.

2. Ziv, A.; Saha, A.; Alpern, H.; Sukenik, N.; Baczewski, L. T.; Yochelis, S.; Reches, M.; Paltiel, Y. AFM-Based Spin-Exchange Microscopy Using Chiral Molecules. *Advanced Materials* **2019**, *31*, 1904206.

3. Bloom, B. P.; Lu, Y.; Metzger, T.; Yochelis, S.; Paltiel, Y.; Fontanesi, C.; Mishra, S.; Tassinari, F.; Naaman, R.; Waldeck, D. H. Asymmetric reactions induced by electron spin polarization. *Physical Chemistry Chemical Physics* **2020**, Advance Article.

4. Metzger, T. S.; Mishra, S.; Bloom, B. P.; Goren, N.; Neubauer, A.; Shmul, G.; Wei, J.;

Yochelis, S.; Tassinari, F.; Fontanesi, C. *et al.* The Electron Spin as a Chiral Reagent. *Angewandte Chemie International Edition* **2020**, *59*, 1653–1658.

5. Mogi, I.; Watanabe, K. Electrocatalytic chirality on magneto-electropolymerized polyaniline electrodes. *Journal of Solid State Electrochemistry* **2007**, *11*, 751–756.

6. Benincori, T.; Arnaboldi, S.; Magni, M.; Grecchi, S.; Cirilli, R.; Fontanesi, C.; Mussini, P. R. Highlighting spin selectivity properties of chiral electrode surfaces from redox potential modulation of an achiral probe under an applied magnetic field. *Chemical Science* **2019**, *10*, 2750–2757.

7. Naaman, R.; Paltiel, Y.; Waldeck, D. H. Chiral molecules and the electron spin. *Nature Reviews Chemistry* **2019**, *3*, 250–260.

8. Tassinari, F.; Steidel, J.; Paltiel, S.; Fontanesi, C.; Lahav, M.; Paltiel, Y.; Naaman, R. Enantioseparation by crystallization using magnetic substrates. *Chem. Sci.* **2019**, *10*, 5246–5250.

9. Ben Dor, O.; Yochelis, S.; Radko, A.; Vankayala, K.; Capua, E.; Capua, A.; Yang, S.-H.; Baczewski, L. T.; Parkin, S. S. P.; Naaman, R. *et al.* Magnetization switching in ferromagnets by adsorbed chiral molecules without current or external magnetic field. *Nature Communications* **2017**, *8*, 14567.

10. Banerjee-Ghosh, K.; Dor, O. B.; Tassinari, F.; Capua, E.; Yochelis, S.; Capua, A.; Yang, S.-H.; Parkin, S. S. P.; Sarkar, S.; Kronik, L. *et al.* Separation of enantiomers by their enantiospecific interaction with achiral magnetic substrates. *Science* **2018**, *360*, 1331–1334.

11. Naaman, R.; Paltiel, Y.; Waldeck, D. H. Chiral Molecules and the Spin Selectivity Effect. *The Journal of Physical Chemistry Letters* **2020**, *11*, 3660–3666.

12. Ray, K.; Ananthavel, S. P.; Waldeck, D. H.; Naaman, R. Asymmetric Scattering of Polarized Electrons by Organized Organic Films of Chiral Molecules. *Science* **1999**, *283*, 814–816.

13. Aragones, A. C.; Medina, E.; Ferrer-Huerta, M.; Gimeno, N.; Teixida, M.; Palma, J. L.; Tao, N.; Ugalde, J. M.; Giralt, E.; Daez-Perez, I. *et al.* Measuring the Spin-Polarization Power of a Single Chiral Molecule. *Small* **2017**, *13*, 1602519.

14. Varade, V.; Markus, T.; Vankayala, K.; Friedman, N.; Sheves, M.; Waldeck, D. H.; Naaman, R. Bacteriorhodopsin based non-magnetic spin filters for biomolecular spintronics. *Physical Chemistry Chemical Physics* **2018**, *20*, 1091–1097.

15. Yeganeh, S.; Ratner, M. A.; Medina, E.; Mujica, V. Chiral electron transport: Scattering through helical potentials. *The Journal of Chemical Physics* **2009**, *131*, 014707.

16. Guo, A.-M.; Sun, Q.-f. Spin-Selective Transport of Electrons in DNA Double Helix. *Physical Review Letters* **2012**, *108*, 218102.

17. Xu, B. Measurement of Single-Molecule Resistance by Repeated Formation of Molecular Junctions. *Science* **2003**, *301*, 1221–1223.

18. Smit, R. H. M.; Noat, Y.; Untiedt, C.; Lang, N. D.; van Hemert, M. C.; van Ruitenbeek, J. M. Measurement of the conductance of a hydrogen molecule. *Nature* **2002**, *419*, 906–909.

19. Venkataraman, L.; Klare, J. E.; Nuckolls, C.; Hybertsen, M. S.; Steigerwald, M. L. Dependence of single-molecule junction conductance on molecular conformation. *Nature* **2006**, *442*, 904–907.

20. Martin, C. A.; Ding, D.; van der Zant, H. S. J.; Ruitenbeek, J. M. v. Lithographic mechanical break junctions for single-molecule measurements in vacuum: possibilities and limitations. *New Journal of Physics* **2008**, *10*, 065008.

21. Xu,; Zhang,; Li,; Tao, Direct Conductance Measurement of Single DNA Molecules in Aqueous Solution. *Nano Letters* **2004**, *4*, 1105–1108.

22. Hihath, J.; Xu, B.; Zhang, P.; Tao, N. Study of single-nucleotide polymorphisms by means of electrical conductance measurements. *Proceedings of the National Academy of Sciences* **2005**, *102*, 16979–16983.

23. Guo, C.; Wang, K.; Zerah-Harush, E.; Hamill, J.; Wang, B.; Dubi, Y.; Xu, B. Molecular rectifier composed of DNA with high rectification ratio enabled by intercalation. *Nature Chemistry* **2016**, *8*, 484–490.

24. Liu, S. P.; Artois, J.; Schmid, D.; Wieser, M.; Bornemann, B.; Weisbrod, S.; Marx, A.; Scheer, E.; Erbe, A. Electronic transport through short dsDNA measured with mechanically controlled break junctions: New thiol-gold binding protocol improves conductance: Electronic transport through short dsDNA. *physica status solidi (b)* **2013**, *250*, 2342–2348.

25. Kawai, K.; Kodera, H.; Majima, T. Long-Range Charge Transfer through DNA by Replacing Adenine with Diaminopurine. *Journal of the American Chemical Society* **2010**, *132*, 627–630.

26. Li, Y.; Arts, J. M.; Demir, B.; Gokce, S.; Mohammad, H. M.; Alangari, M.; Anantram, M. P.; Oren, E. E.; Hihath, J. Detection and identification of genetic material via single-molecule conductance. *Nature Nanotechnology* **2018**, *13*, 1167–1173.

27. Li, Y.; Artes, J. M.; Hihath, J. Long-Range Charge Transport in Adenine-Stacked RNA:DNA Hybrids. *Small* **2016**, *12*, 432–437.

28. Paul, A.; Watson, R. M.; Wierzbinski, E.; Davis, K. L.; Sha, A.; Achim, C.; Waldeck, D. H. Distance Dependence of the Charge Transfer Rate for Peptide Nucleic Acid Monolayers. *The Journal of Physical Chemistry B* **2010**, *114*, 14140–14148.

29. Sek, S.; Misicka, A.; Swiatek, K.; Maicka, E. Conductance of α-Helical Peptides Trapped within Molecular Junctions. *The Journal of Physical Chemistry B* **2006**, *110*, 19671–19677.

30. Xiao, X.; Xu, B.; Tao, N. Changes in the Conductance of Single Peptide Molecules upon Metal-Ion Binding. *Angewandte Chemie International Edition* **2004**, *43*, 6148–6152.

31. Artes, J. M.; Lopez-Martinez, M.; Giraudet, A.; Diez-Perez, I.; Sanz, F.; Gorostiza, P. Current-Voltage Characteristics and Transition Voltage Spectroscopy of Individual Redox Proteins. *Journal of the American Chemical Society* **2012**, *134*, 20218–20221.

32. Zhang, B.; Song, W.; Brown, J.; Nemanich, R.; Lindsay, S. Electronic Conductance Resonance in Non-Redox-Active Proteins. *Journal of the American Chemical Society* **2020**, *142*, 6432–6438.

33. Aragons, A. C.; Aravena, D.; Cerd, J. I.; Acs-Castillo, Z.; Li, H.; Real, J. A.; Sanz, F.; Hihath, J.; Ruiz, E.; Dez-Prez, I. Large Conductance Switching in a Single-Molecule Device through Room Temperature Spin-Dependent Transport. *Nano Letters* **2016**, *16*, 218–226.

34. Osorio, E. A.; Moth-Poulsen, K.; van der Zant, H. S. J.; Paaske, J.; Hedegrd, P.; Flensberg, K.; Bendix, J.; Bjrnholm, T. Electrical Manipulation of Spin States in a Single Electrostatically Gated Transition-Metal Complex. *Nano Letters* **2010**, *10*, 105–110.

35. Duli, D.; Tuukkanen, S.; Chung, C.-L.; Isambert, A.; Lavie, P.; Filoramo, A. Direct conductance measurements of short single DNA molecules in dry conditions. *Nanotechnology* **2009**, *20*, 115502.

36. Artes, J. M.; Li, Y.; Qi, J.; Anantram, M. P.; Hihath, J. Conformational gating of DNA conductance. *Nature Communications* **2015**, *6*, 8870.

37. Adessi, C.; Walch, S.; Anantram, M. P. Environment and structure influence on DNA conduction. *Physical Review B* **2003**, *67*, 081405.

38. Kasumov, A. Y.; Klinov, D. V.; Roche, P.-E.; Guron, S.; Bouchiat, H. Thickness and low-temperature conductivity of DNA molecules. *Applied Physics Letters* **2004**, *84*, 1007–1009.

39. Xiang, L.; Palma, J. L.; Bruot, C.; Mujica, V.; Ratner, M. A.; Tao, N. Intermediate tunnelling-hopping regime in DNA charge transport. *Nature Chemistry* **2015**, *7*, 221–226.

40. Xie, Z.; Markus, T. Z.; Cohen, S. R.; Vager, Z.; Gutierrez, R.; Naaman, R. Spin Specific Electron Conduction through DNA Oligomers. *Nano Letters* **2011**, *11*, 4652–4655.

41. Xiong, Z. H.; Wu, D.; Vardeny, Z. V.; Shi, J. Giant magnetoresistance in organic spin-valves. *Nature* **2004**, *427*, 4.

42. Schmaus, S.; Bagrets, A.; Nahas, Y.; Yamada, T. K.; Bork, A.; Bowen, M.; Beaurepaire, E.; Evers, F.; Wulfhekel, W. Giant magnetoresistance through a single molecule. *Nature Nanotechnology* **2011**, *6*, 185–189.

43. Mishra, S.; Mondal, A. K.; Pal, S.; Das, T. K.; Smolinsky, E. Z. B.; Siligardi, G.; Naaman, R. Length-Dependent Electron Spin Polarization in Oligopeptides and DNA. *The Journal of Physical Chemistry C* **2020**, *124*, 10776–10782.

44. Lu, H.; Wang, J.; Xiao, C.; Pan, X.; Chen, X.; Brunecky, R.; Berry, J. J.; Zhu, K.; Beard, M. C.; Vardeny, Z. V. Spin-dependent charge transport through 2D chiral hybrid lead-iodide perovskites. *Science Advances* **2019**, *5*, eaay0571.

45. Cheung, K. M.; Stemer, D. M.; Zhao, C.; Young, T. D.; Belling, J. N.; Andrews, A. M.; Weiss, P. S. Chemical Lift-Off Lithography of Metal and Semiconductor Surfaces. *ACS Materials Letters* **2020**, *2*, 76–83.

46. Mekhalif, Z.; Riga, J.; Pireaux, J.-J.; Delhalle, J. Self-Assembled Monolayers of n - Dodecanethiol on Electrochemically Modified Polycrystalline Nickel Surfaces. *Langmuir* **1997**, *13*, 2285–2290.

47. Abendroth, J. M.; Nakatsuka, N.; Ye, M.; Kim, D.; Fullerton, E. E.; Andrews, A. M.; Weiss, P. S. Analyzing Spin Selectivity in DNA-Mediated Charge Transfer *via* Fluorescence Microscopy. *ACS Nano* **2017**, *11*, 7516–7526.

48. Abendroth, J. M.; Cheung, K. M.; Stemer, D. M.; El Hadri, M. S.; Zhao, C.; Fullerton, E. E.; Weiss, P. S. Spin-Dependent Ionization of Chiral Molecular Films. *Journal of the American Chemical Society* **2019**, *141*, 3863–3874.

49. Stemer, D. M.; Abendroth, J. M.; Cheung, K. M.; Ye, M.; El Hadri, M. S.; Fullerton, E. E.; Weiss, P. S. Differential Charging in Photoemission from Mercurated DNA Monolayers on Ferromagnetic Films. *Nano Letters* **2020**, *20*, 1218–1225.

50. Mondal, P. C.; Fontanesi, C.; Waldeck, D. H.; Naaman, R. Field and Chirality Effects on Electrochemical Charge Transfer Rates: Spin Dependent Electrochemistry. *ACS Nano* **2015**, *9*, 3377–3384.

51. Ghosh, S.; Mishra, S.; Avigad, E.; Bloom, B. P.; Baczewski, L. T.; Yochelis, S.; Paltiel, Y.; Naaman, R.; Waldeck, D. H. Effect of Chiral Molecules on the Electron's Spin Wavefunction at Interfaces. *The Journal of Physical Chemistry Letters* **2020**, *11*, 1550–1557.

52. Bloom, B. P.; Kiran, V.; Varade, V.; Naaman, R.; Waldeck, D. H. Spin Selective Charge Transport through Cysteine Capped CdSe Quantum Dots. *Nano Letters* **2016**, *16*, 4583–4589.

53. Choi, J. K.; Haynie, B. E.; Tohgha, U.; Pap, L.; Elliott, K. W.; Leonard, B. M.; Dzyuba, S. V.; Varga, K.; Kubelka, J.; Balaz, M. Chirality Inversion of CdSe and CdS

Quantum Dots without Changing the Stereochemistry of the Capping Ligand. *ACS Nano* **2016**, *10*, 3809–3815.

54. Kulkarni, C.; Mondal, A. K.; Das, T. K.; Grinbom, G.; Tassinari, F.; Mabesoone, M. F. J.; Meijer, E. W.; Naaman, R. Highly Efficient and Tunable Filtering of Electrons' Spin by Supramolecular Chirality of Nanofiber-Based Materials. *Advanced Materials* **2020**, *32*, 1904965.

55. Lu, H.; Xiao, C.; Song, R.; Li, T.; Maughan, A. E.; Levin, A.; Brunecky, R.; Berry, J. J.; Mitzi, D. B.; Blum, V. *et al.* Highly Distorted Chiral Two-Dimensional Tin Iodide Perovskites for Spin Polarized Charge Transport. *Journal of the American Chemical Society* **2020**, *142*, 13030–13040.

56. Kaiser, U.; Schwarz, A.; Wiesendanger, R. Magnetic exchange force microscopy with atomic resolution. *Nature* **2017**, *446*, 522–525.

57. Shapira, T.; Alpern, H.; Yochelis, S.; Lee, T.-K.; Kaun, C.-C.; Paltiel, Y.; Koren, G.; Millo, O. Unconventional order parameter induced by helical chiral molecules adsorbed on a metal proximity coupled to a superconductor. *Physical Review B* **2018**, *98*, 214513.

58. Alpern, H.; Yavilberg, K.; Dvir, T.; Sukenik, N.; Klang, M.; Yochelis, S.; Cohen, H.; Grosfeld, E.; Steinberg, H.; Paltiel, Y. *et al.* Magnetic-related States and Order Parameter Induced in a Conventional Superconductor by Nonmagnetic Chiral Molecules. *Nano Letters* **2019**, *19*, 5167–5175.

59. Sukenik, N.; Alpern, H.; Katzir, E.; Yochelis, S.; Millo, O.; Paltiel, Y. Proximity Effect through Chiral Molecules in Nb-Graphene-Based Devices. *Advanced Materials Technologies* **2018**, *3*, 1700300.

60. Dianat, A.; Gutierrez, R.; Alpern, H.; Mujica, V.; Ziv, A.; Yochelis, S.; Millo, O.; Paltiel, Y.; Cuniberti, G. The Role of Exchange Interactions in the Magnetic Response and Inter-Molecular Recognition of Chiral Molecules. *Nano Letters* **2020**, in press.

61. Wu, Y.; Miao, G.; Subotnik, J. Chemical Reaction Rates for Systems with Spin-Orbit Coupling and an Odd Number of Electrons: Does Berry's Phase Lead to Meaningful Spin-Dependent Nuclear Dynamics for a Two State Crossing? **2020**, arXiv preprint arXiv:2005.10424.

62. Göhler, B.; Hamelbeck, V.; Markus, T. Z.; Kettner, M.; Hanne, G. F.; Vager, Z.; Naaman, R.; Zacharias, H. Spin Selectivity in Electron Transmission Through Self-Assembled Monolayers of Double-Stranded DNA. *Science* **2011**, *331*, 894–897.

63. Naaman, R.; Waldeck, D. H. Chiral-Induced Spin Selectivity Effect. *The Journal of Physical Chemistry Letters* **2012**, *3*, 2178–2187.

64. Naaman, R.; Waldeck, D. H. Spintronics and Chirality: Spin Selectivity in Electron Transport Through Chiral Molecules. *Annual Review of Physical Chemistry* **2015**, *66*, 263–281.

65. Carmeli, I.; Skakalova, V.; Naaman, R.; Vager, Z. Magnetization of Chiral Monolayers of Polypeptide: A Possible Source of Magnetism in Some Biological Membranes. *Angewandte Chemie International Edition* **2002**, *41*, 761–764.

66. Ghosh, K. B.; Zhang, W.; Tassinari, F.; Mastai, Y.; Lidor-Shalev, O.; Naaman, R.; Mllers, P.; Nrenberg, D.; Zacharias, H.; Wei, J. *et al.* Controlling Chemical Selectivity in Electrocatalysis with Chiral CuO-Coated Electrodes. *The Journal of Physical Chemistry C* **2019**, *123*, 3024–3031.

67. Wei, J. J.; Schafmeister, C.; Bird, G.; Paul, A.; Naaman, R.; Waldeck, D. H. Molecular Chirality and Charge Transfer through Self-Assembled Scaffold Monolayers. *The Journal of Physical Chemistry B* **2006**, *110*, 1301–1308.

68. Guo, A.-M.; Sun, Q.-F. Spin-dependent electron transport in protein-like single-helical molecules. *Proceedings of the National Academy of Sciences* **2014**, *111*, 11658–11662.

69. Ben Dor, O.; Morali, N.; Yochelis, S.; Baczewski, L. T.; Paltiel, Y. Local Light-Induced Magnetization Using Nanodots and Chiral Molecules. *Nano Letters* **2014**, *14*, 6042–6049.

70. Eckshtain-Levi, M.; Capua, E.; Refaely-Abramson, S.; Sarkar, S.; Gavrilov, Y.; Mathew, S. P.; Paltiel, Y.; Levy, Y.; Kronik, L.; Naaman, R. Cold denaturation induces inversion of dipole and spin transfer in chiral peptide monolayers. *Nature Communications* **2016**, *7*, 10744.

71. Maslyuk, V. V.; Gutierrez, R.; Dianat, A.; Mujica, V.; Cuniberti, G. Enhanced Magnetoresistance in Chiral Molecular Junctions. *The Journal of Physical Chemistry Letters* **2018**, *9*, 5453–5459.

72. Zöllner, M. S.; Varela, S.; Medina, E.; Mujica, V.; Herrmann, C. Insight into the Origin of Chiral-Induced Spin Selectivity from a Symmetry Analysis of Electronic Transmission. *Journal of Chemical Theory and Computation* **2020**, *16*, 2914–2929.

73. Michaeli, K.; Varade, V.; Naaman, R.; Waldeck, D. H. A new approach towards spintronics: spintronics with no magnets. *Journal of Physics: Condensed Matter* **2017**, *29*, 103002.

74. Banerjee, A. S. Ab initio framework for systems with helical symmetry: theory, numerical implementation and applications to torsional deformations in nanostructures. **2020**, arXiv preprint arXiv:2008.02267.

75. Ghosh, S.; Banerjee, A. S.; Suryanarayana, P. Symmetry-adapted real-space density functional theory for cylindrical geometries: Application to large group-IV nanotubes. *Physical Review B* **2019**, *100*, 125143.

76. Lin, L. Adaptively compressed exchange operator. *Journal of chemical theory and computation* **2016**, *12*, 2242–2249.

77. Hu, W.; Lin, L.; Banerjee, A. S.; Vecharynski, E.; Yang, C. Adaptively compressed exchange operator for large-scale hybrid density functional calculations with applications to the adsorption of water on silicene. *Journal of chemical theory and computation* **2017**, *13*, 1188–1198.

78. Santos, J. I.; Rivilla, I.; Cosso, F. P.; Matxain, J. M.; Grzelczak, M.; Mazinani, S. K. S.; Ugalde, J. M.; Mujica, V. Chirality-Induced Electron Spin Polarization and Enantiospecific Response in Solid-State Cross-Polarization Nuclear Magnetic Resonance. *ACS Nano* **2018**, *12*, 11426–11433.

79. Huang, Z.; Bloom, B. P.; Ni, X.; Georgieva, Z. N.; Marciesky, M.; Vetter, E.; Liu, F.; Waldeck, D. H.; Sun, D. Magneto-Optical Detection of Photoinduced Magnetism *via* Chirality-Induced Spin Selectivity in 2D Chiral Hybrid Organic-Inorganic Perovskites. *ACS Nano* **2020**, *14*, 10370–10375.

80. Blumenschein, F.; Tamski, M.; Roussel, C.; Smolinsky, E. Z. B.; Tassinari, F.; Naaman, R.; Ansermet, J.-P. Spin-dependent charge transfer at chiral electrodes probed by magnetic resonance. *Physical Chemistry Chemical Physics* **2020**, *22*, 997–1002.

81. Kurian, P.; Capolupo, A.; Craddock, T.; Vitiello, G. Water-mediated correlations in DNA-enzyme interactions. *Physics Letters A* **2018**, *382*, 33–43.

82. Kondepudi, D. K.; Kaufman, R. J.; Singh, N. Chiral Symmetry Breaking in Sodium Chlorate Crystallizaton. *Science* **1990**, *250*, 975–976.

83. Farago, P. S. Electron optic dichroism and electron optic activity. *Journal of Physics B: Atomic and Molecular Physics* **1981**, *14*, L743–L748.

84. Blum, K.; Thompson, D. Spin-dependent electron scattering from oriented molecules. *Journal of Physics B: Atomic, Molecular and Optical Physics* **1989**, *22*, 1823–1844.

85. Mayer, S.; Kessler, J. Experimental Verification of Electron Optic Dichroism. *Physical Review Letters* **1995**, *74*, 4803–4806.

86. Medina, E.; Gonzlez-Arraga, L. A.; Finkelstein-Shapiro, D.; Berche, B.; Mujica, V. Continuum model for chiral induced spin selectivity in helical molecules. *The Journal of Chemical Physics* **2015**, *142*, 194308.

87. Rosenberg, R. A.; Symonds, J. M.; Kalyanaraman, V.; Markus, T.; Orlando, T. M.; Naaman, R.; Medina, E. A.; Lpez, F. A.; Mujica, V. Kinetic Energy Dependence of Spin Filtering of Electrons Transmitted through Organized Layers of DNA. *The Journal of Physical Chemistry C* **2013**, *117*, 22307–22313.

88. Gutierrez, R.; Daz, E.; Naaman, R.; Cuniberti, G. Spin-selective transport through helical molecular systems. *Physical Review B* **2012**, *85*, 081404.

89. Varela, S.; Mujica, V.; Medina, E. Effective spin-orbit couplings in an analytical tight-binding model of DNA: Spin filtering and chiral spin transport. *Physical Review B* **2016**, *93*, 155436.

90. Bardarson, J. H. A proof of the Kramers degeneracy of transmission eigenvalues from antisymmetry of the scattering matrix. *Journal of Physics A: Mathematical and Theoretical* **2008**, *41*, 405203.

91. Salazar, S. V.; Mujica, V.; Medina, E. Spin-orbit Coupling Modulation in DNA by Mechanical Deformations. *CHIMIA International Journal for Chemistry* **2018**, *72*, 411–417.

92. Geyer, M.; Gutierrez, R.; Mujica, V.; Cuniberti, G. Chirality-Induced Spin Selectivity in a Coarse-Grained Tight-Binding Model for Helicene. *The Journal of Physical Chemistry C* **2019**, *123*, 27230–27241.

93. Varela, S.; Montaes, B.; Lpez, F.; Berche, B.; Guillot, B.; Mujica, V.; Medina, E. Intrinsic Rashba coupling due to hydrogen bonding in DNA. *The Journal of Chemical Physics* **2019**, *151*, 125102.

94. Nitzan, A. Electron transmission through molecules and molecular interfaces. *Annual Review of Physical Chemistry* **2001**, *52*, 681–750.

95. Grib, N. V.; Ryndyk, D. A.; Gutirrez, R.; Cuniberti, G. Distance-dependent coherent charge transport in DNA: crossover from tunneling to free propagation. *Journal of Biophysical Chemistry* **2010**, *01*, 77–85.

96. Marvi, M.; Ghadiri, M. A Mathematical Model for Vibration Behavior Analysis of DNA and Using a Resonant Frequency of DNA for Genome Engineering. *Scientific Reports* **2020**, *10*, 3439.

97. Varela, S.; Zambrano, I.; Berche, B.; Mujica, V.; Medina, E. Spin-orbit interaction and spin selectivity for tunneling electron transfer in DNA. *Physical Review B* **2020**, *101*, 241410.

98. Matityahu, S.; Utsumi, Y.; Aharony, A.; Entin-Wohlman, O.; Balseiro, C. A. Spin-dependent transport through a chiral molecule in the presence of spin-orbit interaction and nonunitary effects. *Physical Review B* **2016**, *93*, 075407.

99. Galperin, M.; Ratner, M. A.; Nitzan, A. Molecular transport junctions: vibrational effects. *Journal of Physics: Condensed Matter* **2007**, *19*, 103201.

100. Suzuura, H.; Ando, T. Phonons and electron-phonon scattering in carbon nanotubes. *Physical Review B* **2002**, *65*, 235412.

101. Woehlecke, M.; Borstel, G. On the Role of Spin-Orbit Coupling and Crystal Symmetry on the Spin-Polarization of Photoelectrons in Nonmagnetic Crystals. *Physica Scripta* **1983**, *T4*, 162–164.

102. Gersten, J.; Kaasbjerg, K.; Nitzan, A. Induced spin filtering in electron transmission through chiral molecular layers adsorbed on metals with strong spin-orbit coupling. *The Journal of Chemical Physics* **2013**, *139*, 114111.

103. Kettner, M.; Maslyuk, V. V.; Nurenberg, D.; Seibel, J.; Gutierrez, R.; Cuniberti, G.; Ernst, K.-H.; Zacharias, H. Chirality-Dependent Electron Spin Filtering by Molecular Monolayers of Helicenes. *The Journal of Physical Chemistry Letters* **2018**, *9*, 2025–2030.

104. Mishra, D.; Markus, T. Z.; Naaman, R.; Kettner, M.; Göhler, B.; Zacharias, H.; Friedman, N.; Sheves, M.; Fontanesi, C. Spin-dependent electron transmission through bacteriorhodopsin embedded in purple membrane. *Proceedings of the National Academy of Sciences* **2013**, *110*, 14872–14876.

105. Kettner, M.; Bhowmick, D. K.; Bartsch, M.; Goehler, B.; Zacharias, H. A Silicon-Based Room Temperature Spin Source without Magnetic Layers. *Advanced Materials Interfaces* **2016**, *3*, 1600595.

106. Mayer, S.; Kessler, J. Experimental Verification of Electron Optic Dichroism. *Phys. Rev. Lett.* **1995**, *74*, 4803–4806.

107. Mayer, S.; Nolting, C.; Kessler, J. Electron scattering from chiral molecules. *Journal of Physics B: Atomic, Molecular and Optical Physics* **1996**, *29*, 3497–3511.

108. Nolting, C.; Mayer, S.; Kessler, J. Electron dichroism - new data and an experimental cross-check. *Journal of Physics B: Atomic, Molecular and Optical Physics* **1997**, *30*, 5491–5499.

109. Alexander, S.; Marciano, A.; Smolin, L. Gravitational origin of the weak interaction's chirality. *Physical Review D* **2014**, *89*, 065017.

110. Bailey, J. Astronomical sources of circularly polarized light and the origin of homochirality. *Origins of Life and Evolution of the Biosphere: The Journal of the International Society for the Study of the Origin of Life* **2001**, *31*, 167–183.

111. Cline, D. B. On the physical origin of the homochirality of life. *European Review* **2005**, *13*, 49–59.

112. Blackmond, D. G. The Origin of Biological Homochirality. *Cold Spring Harbor Perspectives in Biology* **2019**, *11*, a032540.

113. Kurian, P.; Dunston, G.; Lindesay, J. How quantum entanglement in DNA synchronizes double-strand breakage by type II restriction endonucleases. *Journal of Theoretical Biology* **2016**, *391*, 102–112.

114. Celardo, G. L.; Angeli, M.; Craddock, T. J. A.; Kurian, P. On the existence of superradiant excitonic states in microtubules. *New Journal of Physics* **2019**, *21*, 023005.

115. Antipas, G. S. E.; Germenis, A. E. Quantum chemical calculations predict biological function: the case of T cell receptor interaction with a peptide/MHC class I. *Frontiers in Chemistry* **2015**, *3*.

116. Rossjohn, J.; Gras, S.; Miles, J. J.; Turner, S. J.; Godfrey, D. I.; McCluskey, J. T Cell Antigen Receptor Recognition of Antigen-Presenting Molecules. *Annual Review of Immunology* **2015**, *33*, 169–200.

117. Courtney, A. H.; Lo, W.-L.; Weiss, A. TCR Signaling: Mechanisms of Initiation and Propagation. *Trends in Biochemical Sciences* **2018**, *43*, 108–123.

118. Antipas, G. S.; Germenis, A. E. The quantum chemical causality of pMHC-TCR biological avidity: Peptide atomic coordination data and the electronic state of agonist N termini. *Data in Brief* **2015**, *3*, 180–184.

119. Sthr, M.; Tkatchenko, A. Quantum mechanics of proteins in explicit water: The role of plasmon-like solute-solvent interactions. *Science Advances* **2019**, *5*, eaax0024.

120. Goldsmith, M.-R.; George, C. B.; Zuber, G.; Naaman, R.; Waldeck, D. H.; Wipf, P.; Beratan, D. N. The chiroptical signature of achiral metal clusters induced by dissymmetric adsorbates. *Phys. Chem. Chem. Phys.* **2006**, *8*, 63–67.

121. Mukhopadhyay, P.; Zuber, G.; Wipf, P.; Beratan, D. Contribution of a Solute's Chiral Solvent Imprint to Optical Rotation. *Angewandte Chemie International Edition* **2007**, *46*, 6450–6452.

122. Mukhopadhyay, P.; Wipf, P.; Beratan, D. N. Optical Signatures of Molecular Dissymmetry: Combining Theory with Experiments To Address Stereochemical Puzzles. *Accounts of Chemical Research* **2009**, *42*, 809–819.

123. Skourtis, S. S.; Beratan, D. N.; Naaman, R.; Nitzan, A.; Waldeck, D. H. Chiral Control of Electron Transmission through Molecules. *Physical Review Letters* **2008**, *101*, 238103.

124. Bloom, B. P.; Liu, R.; Zhang, P.; Ghosh, S.; Naaman, R.; Beratan, D. N.; Waldeck, D. H. Directing Charge Transfer in Quantum Dot Assemblies. *Accounts of Chemical Research* **2018**, *51*, 2565–2573.

125. Bloom, B. P.; Graff, B. M.; Ghosh, S.; Beratan, D. N.; Waldeck, D. H. Chirality Control of Electron Transfer in Quantum Dot Assemblies. *Journal of the American Chemical Society* **2017**, *139*, 9038–9043.

126. Lloyd, S.; Braunstein, S. L. Quantum Computation over Continuous Variables. *Physical Review Letters* **1999**, *82*, 1784–1787.

127. Flamini, F.; Spagnolo, N.; Sciarrino, F. Photonic quantum information processing: a review. *Reports on Progress in Physics* **2019**, *82*, 016001.

128. Fickler, R.; Lapkiewicz, R.; Plick, W. N.; Krenn, M.; Schaeff, C.; Ramelow, S.; Zeilinger, A. Quantum Entanglement of High Angular Momenta. *Science* **2012**, *338*, 640–643.

129. Forbes, K. A.; Andrews, D. L. Spin-orbit interactions and chiroptical effects engaging orbital angular momentum of twisted light in chiral and achiral media. *Physical Review A* **2019**, *99*, 023837.

130. Pu, M.; Ma, X.; Zhao, Z.; Li, X.; Wang, Y.; Gao, H.; Hu, C.; Gao, P.; Wang, C.; Luo, X. Near-field collimation of light carrying orbital angular momentum with bull's-eye-assisted plasmonic coaxial waveguides. *Scientific Reports* **2015**, *5*, 12108.

131. Gorodetski, Y.; Drezet, A.; Genet, C.; Ebbesen, T. W. Generating Far-Field Orbital Angular Momenta from Near-Field Optical Chirality. *Physical Review Letters* **2013**, *110*, 203906.

132. Schmiegelow, C. T.; Schulz, J.; Kaufmann, H.; Ruster, T.; Poschinger, U. G.; Schmidt-Kaler, F. Transfer of optical orbital angular momentum to a bound electron. *Nature Communications* **2016**, *7*, 12998.

133. Konzelmann, A. M.; Krger, S. O.; Giessen, H. Interaction of orbital angular momentum light with Rydberg excitons: Modifying dipole selection rules. *Physical Review B* **2019**, *100*, 115308.

134. Qiu, D. Y.; Cao, T.; Louie, S. G. Nonanalyticity, Valley Quantum Phases, and Lightlike Exciton Dispersion in Monolayer Transition Metal Dichalcogenides: Theory and First-Principles Calculations. *Physical Review Letters* **2015**, *115*, 176801.

135. Fleming, G. R.; Ratner, M. A. Grand challenges in basic energy sciences. *Physics Today* **2008**, *61*, 28–33.

136. Giusteri, G. G.; Mattiotti, F.; Celardo, G. L. Non-Hermitian Hamiltonian approach to quantum transport in disordered networks with sinks: Validity and effectiveness. *Physical Review B* **2015**, *91*.

137. Celardo, G. L.; Poli, P.; Lussardi, L.; Borgonovi, F. Cooperative robustness to dephasing: Single-exciton superradiance in a nanoscale ring to model natural light-harvesting systems. *Physical Review B* **2014**, *90*.

138. Chávez, N. C.; Mattiotti, F.; Méndez-Bermúdez, J. A.; Borgonovi, F.; Celardo, G. L. Real and imaginary energy gaps: a comparison between single excitation Superradiance and Superconductivity and robustness to disorder. *The European Physical Journal B* **2019**, *92*.

139. Dicke, R. H. Coherence in Spontaneous Radiation Processes. *Physical Review* **1954**, *93*, 99–110.

140. Bonifacio, R.; Lugiato, L. A. Cooperative radiation processes in two-level systems: Superfluorescence. *Physical Review A* **1975**, *11*, 1507–1521.

141. Cong, K.; Zhang, Q.; Wang, Y.; Noe, G. T.; Belyanin, A.; Kono, J. Dicke superradiance in solids [Invited]. *Journal of the Optical Society of America B* **2016**, *33*, C80.

142. Araújo, M. O.; Krešić, I.; Kaiser, R.; Guerin, W. Superradiance in a Large and Dilute Cloud of Cold Atoms in the Linear-Optics Regime. *Physical Review Letters* **2016**, *117*.

143. Monshouwer, R.; Abrahamsson, M.; van Mourik, F.; van Grondelle, R. Superradiance and Exciton Delocalization in Bacterial Photosynthetic Light-Harvesting Systems. *The Journal of Physical Chemistry B* **1997**, *101*, 7241–7248.

144. Boer, S. D.; Wiersma, D. A. Dephasing-induced damping of superradiant emission in J-aggregates. *Chemical Physics Letters* **1990**, *165*, 45–53.

145. Fidder, H.; Knoester, J.; Wiersma, D. A. Superradiant emission and optical dephasing in J-aggregates. *Chemical Physics Letters* **1990**, *171*, 529–536.

146. Scheibner, M.; Schmidt, T.; Worschech, L.; Forchel, A.; Bacher, G.; Passow, T.; Hommel, D. Superradiance of quantum dots. *Nature Physics* **2007**, *3*, 106–110.

147. Brandes, T. Coherent and collective quantum optical effects in mesoscopic systems. *Physics Reports* **2005**, *408*, 315–474.

148. Bradac, C.; Johnsson, M. T.; van Breugel, M.; Baragiola, B. Q.; Martin, R.; Juan, M. L.; Brennen, G. K.; Volz, T. Room-temperature spontaneous superradiance from single diamond nanocrystals. *Nature Communications* **2017**, *8*.

149. Rainò, G.; Becker, M. A.; Bodnarchuk, M. I.; Mahrt, R. F.; Kovalenko, M. V.; Stferle, T. Superfluorescence from lead halide perovskite quantum dot superlattices. *Nature* **2018**, *563*, 671–675.

150. Higgins, K. D. B.; Benjamin, S. C.; Stace, T. M.; Milburn, G. J.; Lovett, B. W.; Gauger, E. M. Superabsorption of light via quantum engineering. *Nature Communications* **2014**, *5*.

151. Hu, X.; Ritz, T.; Damjanović, A.; Schulten, K. Pigment Organization and Transfer of Electronic Excitation in the Photosynthetic Unit of Purple Bacteria. *The Journal of Physical Chemistry B* **1997**, *101*, 3854–3871.

152. Strmpfer, J.; Şener, M.; Schulten, K. How Quantum Coherence Assists Photosynthetic Light-Harvesting. *The Journal of Physical Chemistry Letters* **2012**, *3*, 536–542.

153. Hu, X.; Damjanovi, A.; Ritz, T.; Schulten, K. Architecture and mechanism of the light-harvesting apparatus of purple bacteria. *Proceedings of the National Academy of Sciences* **1998**, *95*, 5935–5941.

154. Sener, M. K.; Olsen, J. D.; Hunter, C. N.; Schulten, K. Atomic-level structural and functional model of a bacterial photosynthetic membrane vesicle. *Proceedings of the National Academy of Sciences* **2007**, *104*, 15723–15728.

155. Bohnet, J. G.; Chen, Z.; Weiner, J. M.; Meiser, D.; Holland, M. J.; Thompson, J. K. A steady-state superradiant laser with less than one intracavity photon. *Nature* **2012**, *484*, 78–81.

156. Kiselev, Y. F.; Prudkoglyad, A.; Shumovskii, A.; Yukalov, V. Detection of superradiant emission from a system of nuclear magnetic moments. *Journal of Experimental and Theoretical Physics* **1988**, *94*, 344–349.

157. Yukalov, V. I. *Nuclear Spin Superradiance*; John Wiley and Sons, 2007.

158. Angerer, A.; Streltsov, K.; Astner, T.; Putz, S.; Sumiya, H.; Onoda, S.; Isoya, J.; Munro, W. J.; Nemoto, K.; Schmiedmayer, J. *et al.* Superradiant emission from colour centres in diamond. *Nature Physics* **2018**, *14*, 1168–1172.

159. Rose, B.; Tyryshkin, A.; Riemann, H.; Abrosimov, N.; Becker, P.; Pohl, H.-J.; Thewalt, M.; Itoh, K.; Lyon, S. Coherent Rabi Dynamics of a Superradiant Spin Ensemble in a Microwave Cavity. *Physical Review X* **2017**, *7*.

160. Li, X.; Bamba, M.; Yuan, N.; Zhang, Q.; Zhao, Y.; Xiang, M.; Xu, K.; Jin, Z.; Ren, W.; Ma, G. *et al.* Observation of Dicke cooperativity in magnetic interactions. *Science* **2018**, *361*, 794–797.

161. Jin, L.; Pfender, M.; Aslam, N.; Neumann, P.; Yang, S.; Wrachtrup, J.; Liu, R.-B. Proposal for a room-temperature diamond maser. *Nature Communications* **2015**, *6*.

162. Breeze, J. D.; Salvadori, E.; Sathian, J.; Alford, N. M.; Kay, C. W. M. Continuous-wave room-temperature diamond maser. *Nature* **2018**, *555*, 493–496.

163. Salvadori, E.; Breeze, J. D.; Tan, K.-J.; Sathian, J.; Richards, B.; Fung, M. W.; Wolfowicz, G.; Oxborrow, M.; Alford, N. M.; Kay, C. W. M. Nanosecond time-resolved characterization of a pentacene-based room-temperature MASER. *Scientific Reports* **2017**, *7*.

164. Zoellner, M. S.; Mujica, V.; Herrmann, C. The Influence of Electronic Structure Modelling and Junction Structure on First-Principles Chiral Induced Spin Selectivity. **2020**, ChemArXiv preprint ChemArXiv:12497690.v1.

165. Dalum, S.; Hedegard, P. Theory of Chiral Induced Spin Selectivity. *Nano Letters* **2019**, *19*, 5253–5259.

166. Ying, L.; Lai, Y.-C. Enhancement of spin polarization by chaos in graphene quantum dot systems. *Physical Review B* **2016**, *93*, 085408.

167. Liu, C.-R.; Chen, X.-Z.; Xu, H.-Y.; Huang, L.; Lai, Y.-C. Effect of chaos on two-dimensional spin transport. *Physical Review B* **2018**, *98*, 115305.

168. Liu, C.-R.; Huang, L.; Luo, H.; Lai, Y.-C. Spin Fano Resonances and Control in Two-Dimensional Mesoscopic Transport. *Physical Review Applied* **2020**, *13*, 034061.

169. Huang, L.; Lai, Y.-C.; Luo, H.-G.; Grebogi, C. Universal formalism of Fano resonance. *AIP Advances* **2015**, *5*, 017137.

170. Huang, L.; Xu, H.-Y.; Grebogi, C.; Lai, Y.-C. Relativistic quantum chaos. *Physics Reports* **2018**, *753*, 1–128.

171. Liu, C.-R.; Huang, L.; Luo, H.; Lai, Y.-C. Spin Fano Resonances and Control in Two-Dimensional Mesoscopic Transport. *Physical Review Applied* **2020**, *13*, 034061.

172. Tian, J.; Hong, S.; Miotkowski, I.; Datta, S.; Chen, Y. P. Observation of current-induced, long-lived persistent spin polarization in a topological insulator: A rechargeable spin battery. *Science Advances* **2017**, *3*, e1602531.

173. Sharma, G.; Economou, S. E.; Barnes, E. Interplay of valley polarization and dynamic nuclear polarization in 2D transition metal dichalcogenides. *Physical Review B* **2017**, *96*, 125201.

174. Zwang, T. J.; Tse, E. C. M.; Zhong, D.; Barton, J. K. A Compass at Weak Magnetic Fields Using Thymine Dimer Repair. *ACS Central Science* **2018**, *4*, 405–412.

175. Kung, H.-H.; Maiti, S.; Wang, X.; Cheong, S.-W.; Maslov, D.; Blumberg, G. Chiral Spin Mode on the Surface of a Topological Insulator. *Physical Review Letters* **2017**, *119*, 136802.

176. Doherty, M. W.; Meriles, C. A.; Alkauskas, A.; Fedder, H.; Sellars, M. J.; Manson, N. B. Towards a Room-Temperature Spin Quantum Bus in Diamond via Electron Photoionization, Transport, and Capture. *Physical Review X* **2016**, *6*, 041035.

177. Tao, L. L.; Tsymbal, E. Y. Persistent spin texture enforced by symmetry. *Nature Communications* **2018**, *9*, 2763.